Relationships of Bedrock Fracturing to Electrical Conductivity and Anisotropy Measurements in a Landfill, Victoria B.C.

by

Gordon Harold James Guy

BScH Geology, Acadia University, 1998

A Thesis Submitted in Partial Fulfillment of the

Requirements for the Degree of

Master of Science

in the

School of Earth and Ocean Sciences

We accept this thesis as conforming to the required standard

[redacted]

Dr. G. Spence, Supervisor (School of Earth and Ocean Sciences)

[redacted]

Dr. M. Best, Member (School of Earth and Ocean Sciences; BeMex Consulting)

[redacted]

Dr. S. Dosso, Department Member (School of Earth and Ocean Sciences)

[redacted]

Mr. N. Lomas, External Member (Capital Regional District, Hartland Landfill)

about a vertical axis and taking readings every 15°. Signal-to-noise was improved by using reciprocity and averaging data separated by 180 or 360°. Results indicate that azimuthal conductivity can vary by as much as 30% between maximum and minimum values. The azimuth of maximum conductivity orientation is approximately 11° ± 51°. The range of maximum conductivities lies within the measured bedrock fracture directions in the area (generally NE-SW, SE-NW, and N-S, i.e. between ± 45°). The EM azimuthal data can be combined with the traditional EM31 data and with GPR, geochemical, and geological sources of data to demonstrate a relationship between electrical anisotropy and subsurface bedrock fracturing.

[redacted]

Dr. G. Spence, Supervisor (School of Earth and Ocean Sciences)

[redacted]

Dr. M. Best, Member (School of Earth and Ocean Sciences; BeMex Consulting)

[redacted]

Dr. S. Dosso, Department Member (School of Earth and Ocean Sciences)

[redacted]

Mr. N. Lomas, External Member (Capital Regional District, Hartland Landfill)

Abstract

Ground conductivity (EM31) and ground-penetrating radar (GPR) surveys were carried out at Hartland Landfill located just north of Victoria, BC, Canada. The bedrock consists mainly of fractured gneiss overlain by a thin layer (up to 2 m thick) of till (Gartner Lee, 1998a). A ground and surface water monitoring program previously indicated that conductive groundwater is flowing south from the leachate collection and containment systems (Gartner Lee, 1998a). The current study was directed at mapping and characterizing the bedrock fracture system which is expected to control the flow of groundwater.

Vertical-dipole EM31 data were collected every 2 m along E-W oriented lines spaced 10 m apart over an area of approximately 195 x 240 m. Several approximately N-S conductive features about 10 to 20 m in width are visible. The conductivity of these features decreases with distance from the landfill (4 mS/m in the north near the Phase 1 landfill to 1 mS/m farther to the south). These N-S conductive features outline the possible direction and extent of conductive groundwater which is flowing away from the landfill. Ground-penetrating radar profiles also show discontinuities near these conductive features, again interpreted as fracturing. In addition, geochemical analyses show higher concentrations of leachate indicators (e.g., conductivity, chloride, ammonia, and iron) closer to the landfill. However, these concentrations have diminished since 1997.

Vertical-dipole azimuthal conductivity data were collected at a number of stations along pre-existing EM lines by rotating the line joining the transmitter and receiver coils

Table of Contents

Abstract ii

Table of Contents iv

List of Tables vi

List of Figures vii

Acknowledgements ix

Chapter

1. Introduction 10

    1.1 Purpose 10

    1.2 Hartland Landfill 11

        1.2.1 Location and History 11

        1.2.2 Bedrock Geology 13

        1.2.3 Hydrogeology 14

        1.2.4 Geochemistry 17

    1.3 Previous Geophysical Work 24

    1.4 Justification and Importance of Thesis Work 25

    1.5 Outline of Thesis 26

2. Theory 27

    2.1 Introduction 27

    2.2 Electromagnetic Methods 27

    2.3 Electromagnetic Azimuthal Methods 35

    2.4 Ground-Penetrating Radar 39

3. Data Collection 42

3.1 Introduction 42

3.2 EM Data 42

3.2.1 Profiles and Contouring 42

3.2.2 Azimuthal Data 52

3.3 GPR Data 55

3.4 Geological Data 57

4. Interpretation and Discussion 60

4.1 Introduction 60

4.2 Electromagnetic Methods 60

4.3 Ground-Penetrating Radar 63

4.4 Geological Data 64

4.4.1 Mineralogy 64

4.4.2 Fracture Detection in Outcrops 64

4.4.3 Geochemistry 65

5. Conclusions 67

References 70

Appendix A. EM Contour Map of all Data 72

Appendix B. Additional EM Azimuthal Data 73

Appendix C. Additional GPR Plots 80

Appendix E. Disc of Additional Data and Thesis back pocket

List of Tables

Table

2.1 Dielectric constants and propagation velocities of radar waves in some geological materials and contaminant fluids 41

3.1 Conductivity measurements taken at the same station in north-south and east-west directions and their observed differences 51

List of Figures

Figure		
1.1	Location map of Hartland Landfill	12
1.2	Plots of conductivity and chloride for monitor well location 3	20
1.3	Plots of conductivity and chloride for monitor well locations 7 and 12	22
1.4	Plots of conductivity and chloride for monitor well location 19	23
2.1	A generalized sketch of an electromagnetic induction prospecting system	29
2.2	Response function versus response parameter	32
2.3	Clay particle with a fixed and a diffuse layer of ions	36
3.1	Location map of EM E-W lines and sampling locations	44
3.2	Coloured EM contour map of apparent conductivities	45
3.3	Stacked EM profiles from Lines 0 S to 100 S	47
3.4	Plot of EM apparent conductivity of Line 20 S which was done twice to investigate repeatability	48
3.5	Location map of EM N-S lines, GPR line, and sampling locations for EM azimuthal data discussed in the text	49
3.6	Plot of EM apparent conductivity in a N-S direction for lines 20 W to 60 W	50
3.7	Comparison of azimuthal conductivities at stations 32 W and 40 W on Line 0 S before and after averaging data 180° apart	53
3.8	Comparison of azimuthal conductivities at stations 36 W and 44 W on Line 0 S before and after averaging of two complete rotations	54
3.9	EM and GPR profile of line 0 S	56
3.10	Rosette diagram indicating main fracture directions in outcrops	58

4.1 Plots of EM azimuthal data at or near the easternmost linear conductor (40 W) 62

4.2 Plot of EM apparent conductivity which intersects monitoring well location 19 66

Acknowledgements

The writer is equally indebted to Dr. Mel Best, Dr. George Spence, and Dr. Stan Dosso. During this study, each in their own way have pushed me to seeing this project to completion. Whether it be funding, endless assistance, or positive reinforcement, they were all instrumental in helping me finish this thesis. I appreciate you all for suggesting me to continue my studies. This project has truly been a learning experience in more ways than one.

This study would not have been possible without the generous support of Geonics Ltd. who provided the EM31 equipment free of charge. As well, Sensors & Software Inc. provided GPR equipment at reduced rental rates. This thesis would also not have been possible without generous support from NSERC.

Special thanks are extended to Mr. Nigel Lomas and other employees of the CRD for generously providing important background information, assistance, and access to the Hartland Landfill site. Field work at Hartland Landfill would not have been possible without the aid of field assistants Michelle Watson, Saz Yaqzan, and Tina Solhart. On several occasions, you all went well out of your way to help me during data collection. As well, I would like to thank Sussi Arason who aided and guided me through all the red tape.

On a personal note, I would like to thank all those people who have supported me during this process. Your support was the driving force that made all the little successes seem so important and all the little failures seem not to matter. Thank you.

CHAPTER 1

Introduction

1.1 Purpose

The purpose of the research reported in this thesis is to apply geophysical, geological, hydrogeological, and geochemical studies to map bedrock fractures containing leachate and/or alteration products at and near a major landfill site. Hartland Landfill is located approximately 14 km outside Victoria, British Columbia. The landfill itself sits on fractured bedrock with no more than 2 m of glacial till overlying it (Gartner Lee, 1998a). These fractures, at least in part, determine the amount and direction of groundwater and leachate movement. Consequently, determining the location and direction of bedrock fractures is essential for understanding the flow regime of the area as well as predicting the optimal location of domestic and monitoring wells.

To map these subsurface fractures, a small area (195 x 240 m) south and down-gradient from the landfill was chosen. A number of geophysical methods were applied, supplemented by geological, hydrogeological, and geochemical data. Geophysical methods included a ground conductivity (EM31) survey and a ground-penetrating radar (GPR) survey to map fractures containing leachate and/or alteration products. In addition, vertical-dipole azimuthal conductivity data were collected as part of the EM31 survey to investigate the use of azimuthal conductivity for mapping subsurface fracture orientations.

Hence this study was undertaken to:

(1) identify flow paths for groundwater,

(2) locate subsurface fractures using electromagnetic, ground-penetrating radar, and geological techniques,

(3) determine if vertical-dipole azimuthal conductivity data aids in fracture detection,

(4) provide suggestions and/or remediation plans for Hartland Landfill,

(5) provide constraints on drilling locations for new monitoring wells.

1.2 Hartland Landfill

1.2.1 Location and History

The Hartland Municipal Landfill is located in the bedrock highlands, about 14 km northwest of Victoria, British Columbia, Canada (Fig. 1.1). This landfill has been in continuous operation since the 1950's and is now the principal waste disposal site for greater Victoria (Gartner Lee, 1998a). Hartland Landfill began operation in 1959, and at that time was privately operated by the Victoria Disposal Company. In 1976 the property was purchased by the Capital Regional District (CRD). Since 1985, Hartland Landfill has been operated by the CRD and is presently the only active landfill in the district which serves as the primary waste disposal for approximately 300 000 people (Gartner Lee, 1998a). The entire Hartland Landfill consists of several parcels of land for a total area of 124 hectares. Only one valley on that land has been used for the actual placement of landfill material. This valley, including Phases 1 and 2 of the landfill, covers approximately 50 hectares (Fig. 1.1; Lomas, 1990). The original landfill area (Phase 1) reached capacity in 1996 and was subsequently capped by an impermeable

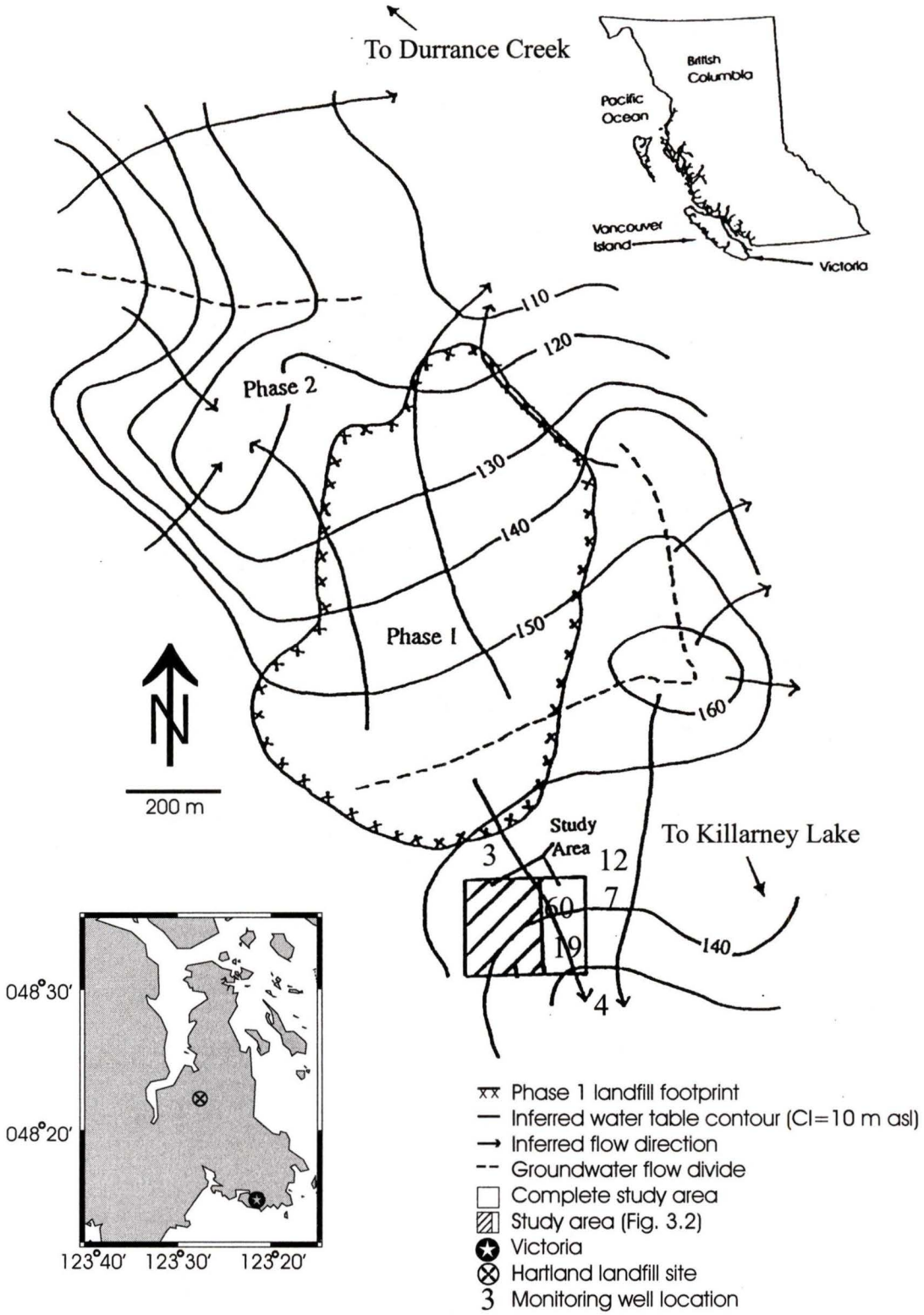

Figure 1.1. Location of Hartland Landfill. Map shows position of capped landfill (Phase 1) as well as inferred water table contours, flow directions, groundwater divides, and monitor well locations. Boxed region indicates location of study where the shaded section of that box represents the portion of the study area corresponding to Fig. 3.2. See disc at back of thesis for coordinates of all monitoring well locations and Appendix A for coordinates and positions of wells 19 and 60 in the study area (Gartner Lee, 1999).

PVC membrane during the summer months from 1997 - 2000. At that time, a new landfill (Phase 2), located just west of Phase 1, commenced operation. This phase will be considerably larger than the original landfill and is expected to supply the needs for the Victoria region for the next 45 years or more (Gartner Lee, 1999).

Throughout the years important modifications have been made to the landfill to improve the environment of the area. These include the addition of leachate collection and containment systems, leachate pipelines, recycling/composting, gas collection, and the capping of Phase 1. As well, a clay berm was constructed along the southern edge of Phase 1 to direct more groundwater flow towards the leachate collection and containment systems to the north (Lomas, 1990).

1.2.2 Bedrock Geology

The bedrock in the Hartland area is mainly comprised of Paleozoic Wark Diorite Gneiss which was metamorphosed during the Jurassic Period. The diorite gneiss is dark green to black in colour. It is generally competent, except in local shear zones, where weathering to clay and chloritization is prominent. Discontinuities, including shear zones, fractures, joints, and altered veins are ubiquitous in bedrock outcrops. (Gartner Lee, 1998a).

Bedrock outcrops are common. In localities where bedrock is not exposed, only a thin veneer of glacial till composed of silty, gravelly sand, with minor cobbles and boulders overlays the gneiss. Minor fluvial deposits consisting of well sorted sands and gravels are present in localized bedrock depressions and channels (Gartner Lee, 1998a).

The entire region has been extensively glaciated in the past, with glacial scouring evident throughout the site area. The result is a characteristic hummocky bedrock topography, along with scour channels and bedrock depressions, normally coinciding with localized faulting, fractures, and joint planes (Piteau et al., 1983).

There is a fairly consistent pattern of predominant structural lineaments oriented approximately N-S. A major fault zone trending N-NE intersects the western boundary of the landfill site as well. Cross faults are also inferred and the surrounding area appears to be regularly faulted, thus creating regional, three-dimensional groundwater flow systems (Piteau et al., 1983).

1.2.3 Hydrogeology

As previously mentioned, the landfill site is divided into two distinct areas referred to as Phase 1 and Phase 2 (Fig. 1.1). Groundwater flow, controlled mostly by topographic relief, is predominantly towards the north where it is collected in a leachate lagoon located on the northern perimeter of the Phase 1 landfill. Leachate is collected in the lagoon and delivered to a sewer system by a collecting pipeline. However, a groundwater flow divide is located approximately 200 m north of the clay berm which marks the southern boundary of the Phase 1 landfill. This divide causes some southward flow of groundwater away from the leachate lagoon and towards the present study area. This study area is 195 m (N-S) x 240 m (E-W), approximately 300 m from the groundwater divide and 100 m from the edge of the Phase 1 footprint. Of this area, most data collection and interpretation is focussed to the west in an area of 195 x 140 m.

The terrain surrounding the landfill is moderately rugged with relief up to 445 m, with the landfill situated in a N-S trending bedrock saddle. Mount Wark lies to the west of the landfill and a bedrock knoll lies to the east. The crest of the landfill forms a drainage divide to the north (flowing towards Durrance Creek) and the southern Killarney Creek drainage basins (Fig. 1.1; Gartner Lee, 1999).

Substantial precipitation in the area allows water to percolate through the Phase 1 landfill into the underlying fractured bedrock. This water leaches out ions (dissolved solids) as it passes through the landfill, forming a leachate which enters the bedrock through fractures, joints, and shear zones and mixes with the groundwater. This contaminated groundwater mixture or leachate travels in the direction of groundwater flow. After the Phase 1 landfill was capped, the amount of water percolating through Phase 1 decreased, however, leachate will continue to flow for several decades after closure. Leachate was detected in monitoring wells located south of Phase 1 in the southeast corner of the study area. Several domestic groundwater wells down-gradient of the monitoring wells were subsequently sealed, and the residents' water supply was replaced with a piped water supply from the Victoria water system (Gartner Lee, 1999).

Groundwater flow in Hartland Landfill is predominantly confined to the fractured bedrock. A few local areas exist where thin veneers of unconsolidated sediments allow groundwater flow down-gradient into creeks within the drainage basins. Vertical flow within these local aquifers also provides a path for surface water to enter the fractured bedrock aquifer (Gartner Lee, 1998a). Direction and rate of groundwater flow in the bedrock is controlled by topography as well as the direction of continuous bedrock fractures (including joints and shear zones) and the fracture density (number of fractures

per unit of surface area). Consequently, information on the direction and density of dominant fractures is essential in order to understand groundwater flow within the bedrock.

Some fractures do not have openings large enough to allow groundwater flow while others are isolated and not connected to other fracture sets. Substantial groundwater will not flow through these discontinuous systems. On the other hand, there may be fractures that are open and connected to other open fractures. These would form continuous flow paths for groundwater. Water moving through these open, connected fractures can interact with minerals on the fracture surfaces to produce a zone of interaction several centimeters thick, thus allowing alteration products (clays and other minerals) to form. These alteration products may also be a result of deformation events related to fracturing and later circulation of hydrothermal fluids as evidenced by vein-filled fractures at the surface. In any case, these alteration zones (as well as the leachate itself) have different physical properties than the surrounding bedrock, permitting geophysical methods to map these zones.

The CRD established a water sampling and geochemical analysis program which was designed to achieve three distinct goals: first, to determine whether or not landfill leachate is infiltrating fractured bedrock; second, to determine if the leachate is in steady-state condition; and third, to determine the amount of dilution and probable future movements of leachate (Gartner Lee, 1998a).

To date, the monitoring program has concluded that leachate does travel through the permeable bedrock and that leachate plumes are present. Movements appeared only

to be moving in N-S directions, towards the leachate lagoon in the north and to the south (Gartner Lee, 1998a), through our area of study.

Leachate analyses from the collection systems met CRD Sewer Use Bylaw Criteria concentrations except for sulphide on six occasions and COD (Carbon Oxygen Demand), BOD (Biological Oxygen Demand), manganese and toluene concentrations on one occasion in 1998. Leachate concentrations were somewhat variable during the 1990's due to dilution from water introduced during Phase 2 construction activities. Average annual leachate flows decreased to 9.8 L/s in 1998 from 15.5 L/s in 1997, due to the capping of Phase 1 and dry summer weather in 1998 (Gartner Lee, 1999).

Groundwater properties appear to be stabilizing, possibly due to operational changes at the site. However, monitoring wells show parameters such as conductivity and concentrations of ammonia, iron, manganese, chloride, tannin, lignin, and others are still above background conditions. According to geochemical measurements, no domestic wells surrounding Hartland Landfill are currently being affected by landfill leachate (Gartner Lee, 1999).

1.2.4 Geochemistry

Groundwater and surface water quality in the vicinity of Hartland Landfill have been monitored since 1983. Annual monitoring reports, presenting interpretations of the impact of landfill leachate on ground and surface water, have been issued since 1988.

The 1998/1999 monitoring program at Hartland Landfill consisted of the following:

- monthly groundwater level measurements,

- continuous water level monitoring using transducers,
- four times per year sampling and laboratory chemical analysis of samples from groundwater monitoring wells and surface water stations,
- three times per year sampling of selected residential wells located in close proximity to the landfill plus one time per year for residential wells within a 2 km radius of the landfill,
- four times per year testing of leachate for Priority Pollutants,
- monthly testing of combined leachate for CRD Sewer-Use Bylaw parameters (Gartner Lee, 1999).

Surface water, groundwater, and leachate sampling as well as groundwater level measurements are carried out by CRD staff and the testing of the samples is conducted by an independent laboratory. Each year, Gartner Lee Ltd. prepares a report on the Hartland Landfill Monitoring Program from the data collected. This annual report presents their interpretations of the impact of Hartland Landfill on surface and groundwater resources based on the monitoring data (Gartner Lee, 1998a;1999).

Conductivity is a good general indicator of inorganic concentrations and a good indicator of leachate contamination. Geochemistry from Hartland Landfill has shown that a plume is present more than 30 m deep at the north toe of the landfill. Dilute leachate, represented by conductivity values between 0.5 and 1 mS/m (5 and 10 μS/cm), has been detected approximately 110 m north of the lower leachate lagoon and into our study area, about 200 m past the southern end of Phase 1 (Gartner Lee, 1999).

Monitoring well locations 3, 4, 7, 12, 19, and 60 are all located south of the Phase 1 landfill (Fig. 1.1). At location 3, water quality in monitor 3-1-3, near the south end of the landfill, has been affected by leachate and had steadily increasing electrical conductivity, chloride, and ammonia values from 1986 to 1995. Concentrations appear to be gradually decreasing since 1995 (Fig. 1.2). However, in 1998, concentrations of chloride, iron and ammonia in this well continued to frequently exceed the respective water quality criteria (B.C. Water Quality Guidelines for Drinking and Recreational Water Uses; B.C. Environment, 1998). Leachate impacts in this shallow well (7 m deep) are the highest detected at any location outside the landfill footprint (Gartner Lee, 1999).

Water quality in the deeper monitoring wells 3-1-1 (26 m deep) and 3-1-2 (16.3 m deep) appear to be only slightly impacted by landfill leachate with much lower values of conductivity, chloride and ammonia. In 1998, conductivity values at these depths appear to be trending slightly lower but chloride concentrations appear to be increasing slightly, as illustrated on Figure 1.2. As well, iron concentrations consistently exceeded water quality criteria (B.C. Environment, 1998) in these two wells in 1998. New monitoring well 3-2-1 (with a larger diameter well casing), located near old location 3, also shows the effects of leachate impact. Conductivity, chloride, and iron concentrations are lower than at well 3-1-3 but are still significantly elevated. Ammonia concentrations in well 3-2-1 are even higher than well 3-1-3 for November 1998 and exceed the freshwater aquatic life criteria (B.C. Criterion for freshwater aquatic life; B.C. Environment, 1998).

Water quality results since 1994 indicate that leachate impacts at wells 7 and 12 have increased substantially since the late 1980's. In 1998, ammonia concentrations in well 12 exceeded criteria on a regular basis. The chloride criterion (B.C. Water Quality

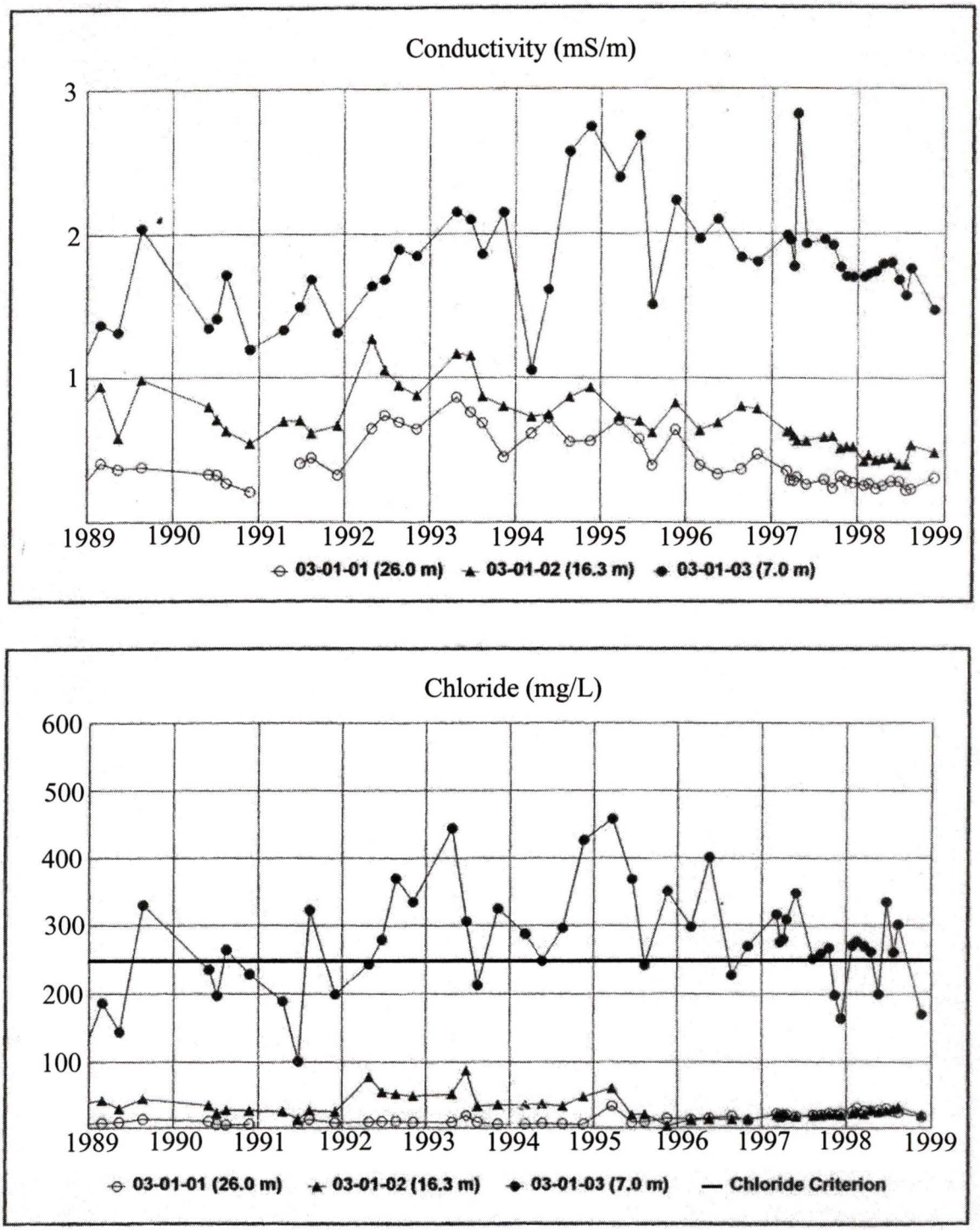

Figure 1.2. Plots of conductivity and chloride versus time for monitoring well location 3 1989 to 1999 (Gartner Lee, 1999).

Guidelines for Drinking and Recreational Water Uses; B.C. Environment, 1998) was exceeded on three dates (Fig. 1.3). In addition, monitoring well 12 is a dugwell which is subject to contamination from surface sources (i.e., Hartland Ave.). In well 7, elevated chloride, conductivity, sodium, and sulphate were detected consistently as in previous years but none of the tested parameters exceeded the criteria (Gartner Lee, 1999).

There are three monitoring wells at location 60 : 60-1-1 (23 m), 60-2-1 (16 m), and 60-3-1 (8 m). Elevated conductivity, chloride, sodium, and sulphate concentrations were present in November 1998 samples at all three depths. However, water quality is better than at location 3 and no water quality criteria were exceeded for the parameters tested (Gartner Lee, 1999).

Sites 4 and 19 are located farther to the south of the landfill (Fig. 1.1). At location 19, water quality is considerably better than at wells closer to the landfill. The water quality in the deep wells (42 and 30 m deep) showed slight leachate impacts in 1995 (Fig. 1.4) but in recent years, concentrations of most parameters declined almost to background levels. Iron concentrations in the two deep monitors exceeded the criterion in 1998 as they did in 1996 and 1997 (Gartner Lee, 1999). However, increases in iron may be caused by the geology rather than influences of contaminated groundwater.

Location 4 is the most southernly groundwater monitor at the landfill. The two deep wells (42 and 30 m deep) at this location have water quality similar to background. In 1996, water quality in the two shallower wells (6 and 11 m deep) had slightly elevated conductivity and chloride levels and exceeded the iron criterion on a few occasions. In 1997 chloride and conductivity levels were similar to 1996 but iron concentrations met the criterion on all sampling dates. Conductivity and chloride concentrations were

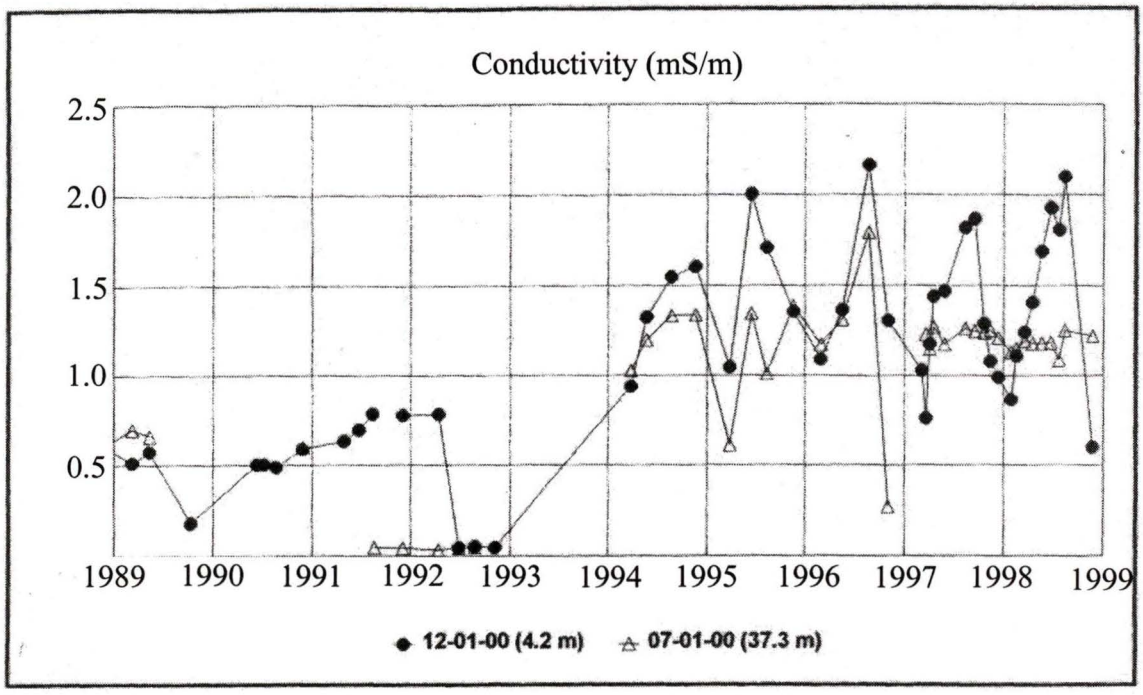

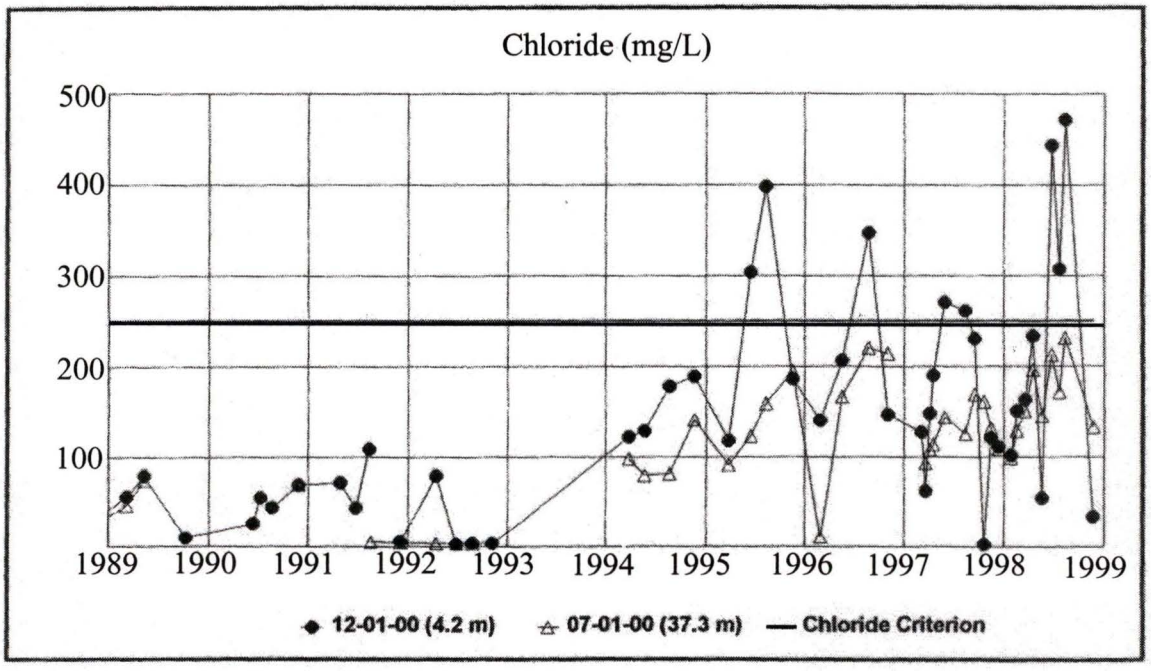

Figure 1.3. Plots of conductivity and chloride versus time for monitor well locations 7 and 12 from 1989 to 1999 (Gartner Lee, 1999).

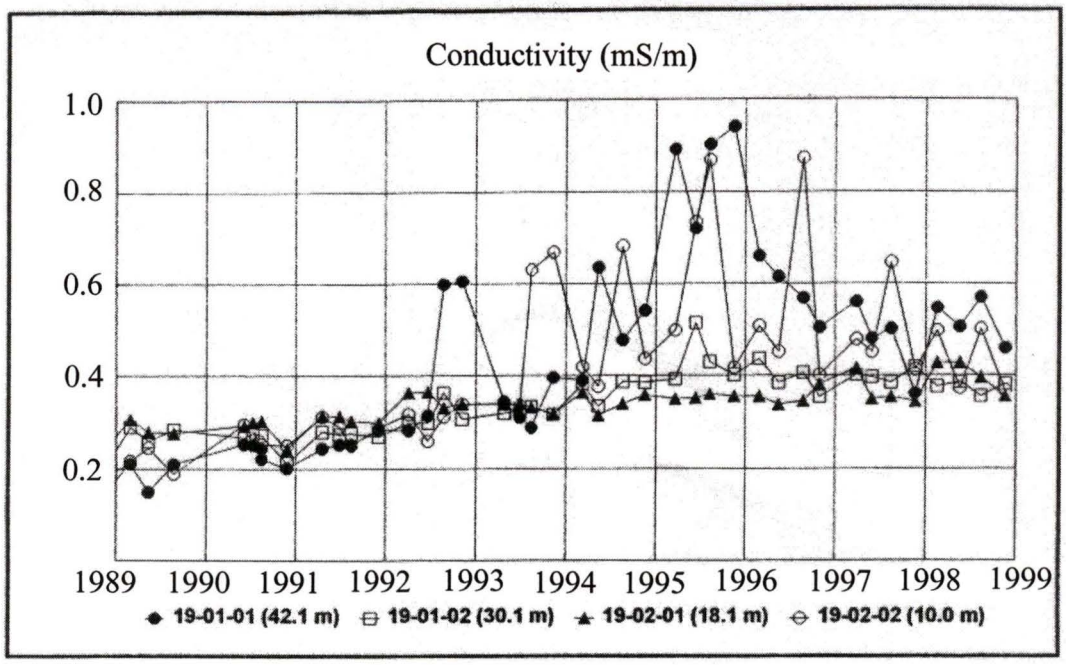

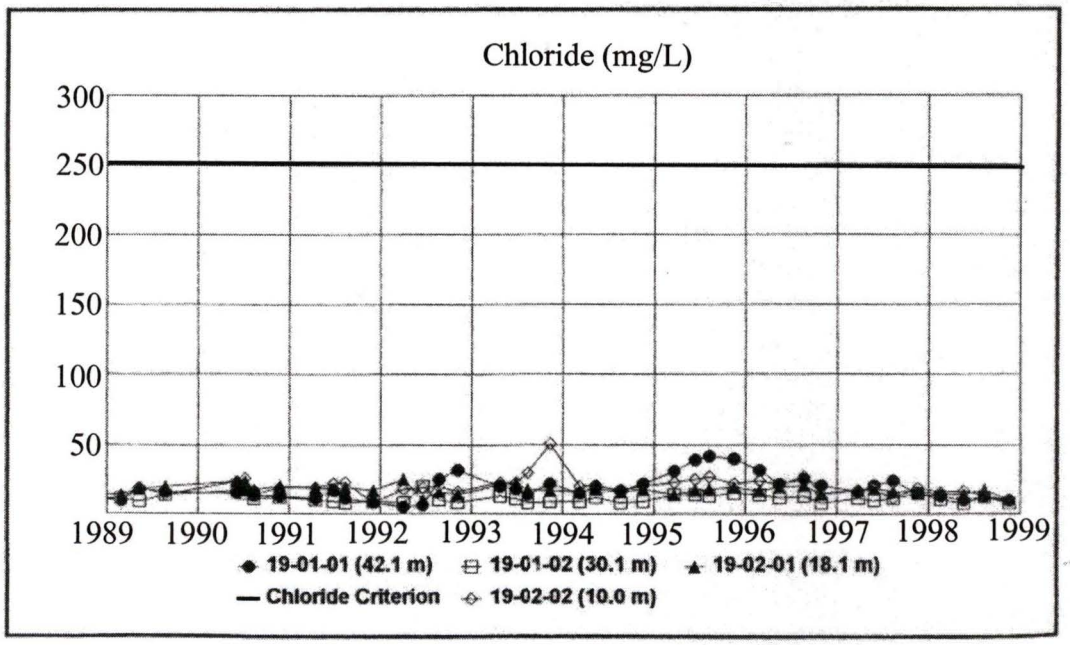

Figure 1.4. Plots of conductivity and chloride versus time for monitor well location 19 from 1989 to 1999 (Gartner Lee, 1999).

slightly higher in 1998 and the iron criteria was exceeded in monitor well 4-1-2 in three of the four 1998 samples. The three new monitoring wells at this location (4-2-1, 4-3-1, and 4-4-1) did not exceed any criteria in the December 1998 sample but the intermediate depth well had chloride and conductivity values that are above background (Gartner Lee, 1999).

1.3 Previous Geophysical Work

In addition to this water monitoring program, an EM31 investigation was also completed in 1997 by Gartner Lee Ltd. to identify the location and extent of any leachate-impacted groundwater downgradient from the landfill. The geophysical survey was completed in an east-west direction, along lines that generally ran west of the access road and extended from the east property boundary to 400 m west of that boundary. A north-south base line was established along a powerline access road which spanned the entire survey area, from near the entrance to 300 m south of the landfill. Although the previous work covers a greater area than the present study, the line spacing used in the 1997 study was much larger (40 m compared to our 10 m); however, the station spacing used was smaller (1 m compared to our 2 m; Gartner Lee, 1998b). Because of the large line spacing, it was not possible to detect finer scaled features such as fractures.

Background conductivity values in this area range from 0 to 4 mS/m. In some areas, conductivity values reach over 100 mS/m. Based on the in-phase results and observations in the field, various landfill infrastructures (metallic objects and powerlines) are a possible source of these conductivity highs. With such a large line spacing, it is difficult to interpret slight changes in conductivity (from 0 to 4 mS/m). It is therefore

believed that increases in conductivity near the Phase 1 landfill may in part be due to leachate impacted groundwater, but no definite plume was observed from the landfill area. Overall, this survey did not clearly identify leachate impacted groundwater in the survey area (Gartner Lee, 1998b).

1.4 Justification and Importance of Thesis Work

The ground and surface water monitoring program for Hartland Landfill has shown that some contaminant has been diverted from the leachate collection and containment systems but still within the property (Gartner Lee, 1998a). Since very little overburden is present, most contaminant is suspected to be travelling through the fractured bedrock on which the landfill sits. It is of great interest to Hartland Landfill staff to be able to map these fractures in order to stop or remediate the flow of further contaminant. This information could also help protect the domestic wells of nearby inhabitants from contamination. In addition, this study could provide information on leachate flow rates by repeating the EM surveys in a few years as well as locating better monitoring well locations.

In this thesis, EM31, GPR, and geological studies are used to aid in the detection and mapping of subsurface fractures. An innovative technique to map fracture orientations is the measurement of conductivities at different azimuths. Azimuthal conductivity measurements are similar to DC azimuthal resistivity measurements, where the objective is to map the maximum (and minimum) conductivity and relate these to electrical anisotropy (Taylor and Fleming, 1988). Therefore, the objective is to determine the directions of maximum (in our case) conductivity and correlate these with

the direction of fracturing in the bedrock. However, little work has been carried out to prove that this method works well for determining the presence and orientations of these subsurface fractures (Slater et al., 1998). We hope to show that these azimuthal conductivity measurements, when integrated with other data sets, can determine subsurface fracture orientations.

1.5 Outline of Thesis

After a brief introduction to this thesis and to the Hartland Landfill (above), the following will be discussed. Chapter 2, Theory, will concentrate on electromagnetic methods, and how the EM31 is able to measure and record apparent conductivities. This same theory will then be adapted to perform EM azimuthal surveys to gain more information on fracture orientation and anisotropy. Basic theory on GPR will then be discussed as the technique will be used later to complement the EM work. Chapter 3, Data Collection, begins with the presentation of EM31 vertical-dipole data as a contour map and as E-W and N-S profiles. Azimuthal data will then be presented on polar plots, followed by GPR profiles and geological data. Chapter 4, Interpretation and Discussion, begins with the analysis of EM data, both traditional and azimuthal. These, along with GPR and geological data, will demonstrate a relationship between electrical anisotropy and bedrock fracturing. Conclusions are then presented in Chapter 5.

CHAPTER 2

Theory

2.1 Introduction

Geophysical approaches can provide fast, economic, and non-invasive ways to study groundwater contamination. Geological, hydrogeological, and geochemical data are not always sufficient in compiling a complete story of the subsurface. However, the addition of geophysics to these other data sets is generally much more informative.

There have been growing concerns that landfills may, in general, be contaminating the groundwater of near-by domestic wells. Since most groundwater flow in the Hartland area occurs through fractured bedrock, a geophysical study was carried out over a very small area to map these potentially conductive groundwater paths with electromagnetic (EM) techniques. To provide independent information on fracture occurrence, ground-penetrating radar (GPR) profiles were used to help interpret the EM data.

2.2 Electromagnetic Methods

Frequency-domain EM surveys are often used to map shallow bedrock fractures and shear zones. Typical systems include the Geonics EM34 and Geonics EM31 systems (McNeill, 1980) as well as the Apex MaxMin system (Best and Boniwell, 1989) with a transmitter-receiver spacing of less than 50 m.

These systems are often used by geophysicists for fracture mapping. The EM31, a frequency domain EM system, maps variations in ground conductivity using a patented EM inductive technique without electrodes or ground contact. With this inductive method, surveys can be carried out under most geological conditions including those of high surface resistivity. The effective depth of exploration is about 6 m (vertical-dipole mode) and approximately 3 m in the horizontal-dipole mode, making it ideal for many geotechnical and groundwater contaminant surveys. We will concentrate on the vertical-dipole mode since its depth of exploration is greater (McNeill, 1980). Important advantages of the EM31 over conventional resistivity methods are the speed with which surveys can be conducted, the precision with which small changes in conductivity can be measured, and the continuous readout and data collection while traversing the survey area (McNeill, 1980). Because of these benefits, the EM31 was used at the Hartland Landfill site. It should also be noted that the limitations of this instrument include its inability to distinguish conductivity highs as being caused by leachate and/or clays as well as being susceptible to recording landfill infrastructures such as metallic objects and powerlines.

EM methods map variations in conductivity within the Earth's surface (Best, 1989). A generalized sketch of an electromagnetic prospecting system exhibits the general principle of electromagnetic surveying (Fig. 2.1). Primary (P) electromagnetic fields are generated by passing alternating current (for frequency domain methods) through a small coil made of multiple turns of wire. These primary electromagnetic fields travel via diffusion from the transmitter coil to the receiver coil. They diffuse out in all directions, both above and below the Earth's surface. If a conducting body is present in the subsurface, the electromagnetic field induces eddy currents to flow in the

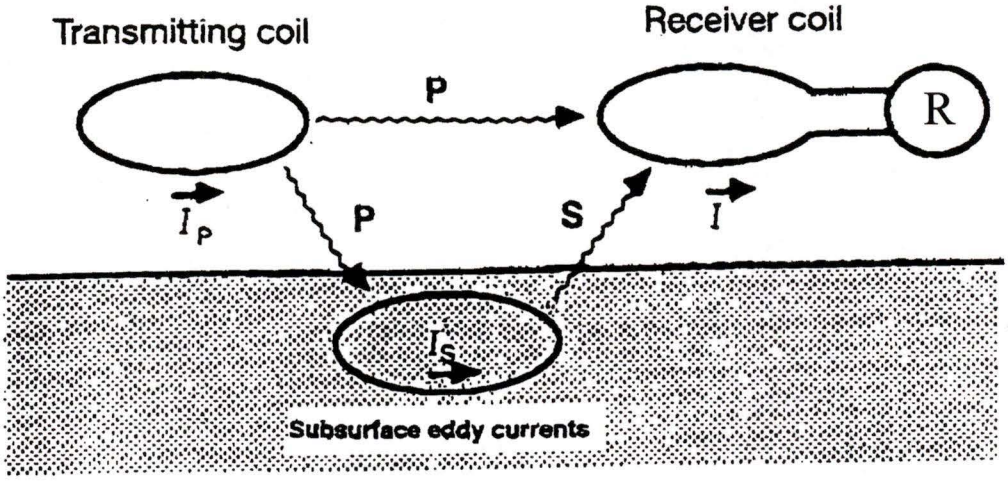

Figure 2.1. A generalized sketch of an electromagnetic induction prospecting system. The transmitting coil, energized with an alternating current (Ip), produces a primary field which induces eddy currents (Is) in the subsurface conductor. The receiver coil measures the resultant R of the primary field (P) and the secondary field (S) induced by the eddy currents (Sharma, 1997).

conductor. These eddy currents will then generate secondary (S) electromagnetic fields which also diffuse in all directions. The receiver measures both primary and secondary electromagnetic field signals. Since the two electromagnetic fields (primary and secondary) were produced by two different currents, their amplitude and phase will differ. It is these differences which reveal the presence of conductive material and can also provide quantitative information on its geometry and electrical properties (Kearey and Brooks, 1991). It is therefore the objective of an EM survey to measure the secondary EM fields and use their deviations from the primary EM fields to deduce the properties of subsurface conductors which produced them (Best, 1989).

The ratio of secondary to primary voltages (V_s/ V_p) depends on the EM coupling between transmitter, receiver, and the earth in a complex way. To reiterate this concept, a three loop system representing a transmitter, receiver, and a conducting loop to represent a finite geological conductor can be used. The ratio of V_s to V_p depends on the coupling between the transmitter-receiver, transmitter-loop, loop-receiver, and the self-inductance of the loop (L). It also depends on the response function F where:

$$F = (\alpha^2 + i\alpha)/(1 + \alpha^2) \qquad (2.1)$$

in which:

$$\alpha = \omega L/R \qquad (2.2)$$

depends on the loop resistivity R, loop self-inductance L, and frequency ω where ω is $2\pi f$ with f being the frequency in Hz. The parameter α is called the response parameter and is a measure of the "goodness" of a conductor at a specific frequency (Best, 1989). More generally, α can be written as:

$$\alpha = \mu\omega\sigma(\text{length})^2 \qquad (2.3)$$

where μ is the magnetic permeability, σ is the conductivity, and the length factor depends on the particular EM configuration being used (Best, 1989).

To illustrate, Figure 2.2 is a plot of the response function versus the response parameter. The real part ($X = \alpha^2/(1+\alpha^2)$) is called the in-phase component and is in-phase with the primary current in the transmitter. The imaginary part ($Y = \alpha/(1 + \alpha^2)$) is called the quadrature component, and is exactly 90° out of phase with the primary current. The phase angle ϕ between these two components is:

$$\tan\phi = Y/X = \alpha/\alpha^2 = 1/\alpha = R/\omega L = 1/\mu\omega\sigma(\text{length})^2 \qquad (2.4)$$

This expression and Figure 2.2 indicate that for small values of Y/X, i.e. large values of α, the phase angle will be small. Therefore small phase angles can indicate the presence of good conductors since σ must be large (assuming ω and the length are fixed such as in the case of the EM31 system). This expression and diagram indicates that the smaller the Y/X ratio, the smaller the phase angle will be. Smaller Y/X ratios and therefore smaller phase angles indicate the presence of good conductors (Sharma, 1997).

$$X = \alpha^2/(1 + \alpha^2)$$

$$Y = \alpha/(1 + \alpha^2)$$

$$\alpha = \omega L/R$$

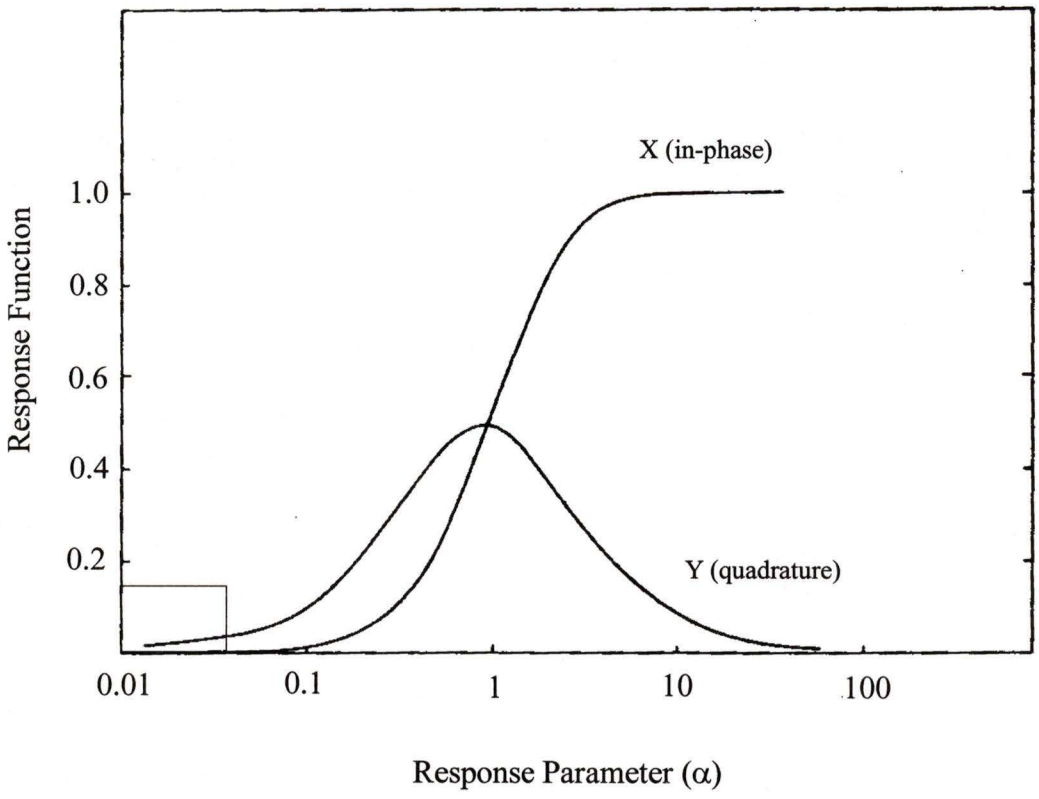

Figure 2.2. Response function versus response parameter (Best, 1989). Boxed area in corner represented low induction numbers where conductivity can be estimated (McNeill, 1980).

For a homogeneous earth of conductivity σ, the response parameter is $\alpha = \mu\omega\sigma(\text{length})^2$ where length is the transmitter-receiver separation. For α very small, the in-phase value (which is an algebraic expression that depends on α) approaches zero and the quadrature value Y (which is also an algebraic expression of α) approaches:

$$Y = \mu\omega\sigma(\text{length})^2/4 \qquad (2.5)$$

Solving for σ yields the following expression which provides a relationship between the quadrature component Y and conductivity where:

$$\sigma = 4Y/\mu\omega(\text{length})^2 \qquad (2.6)$$

Small values of α imply small values of $\mu\omega\sigma(\text{length})^2$. For the EM31 system, length is 3.66 m and f = 9800 Hz. For μ equal to the free space value of $4\pi \times 10^{-7}$ H/m we find $\alpha = 1.04\sigma$ which, for values of σ smaller than 0.1 S/m (100 mS/m) can be considered small. Larger values of σ require a correction which has been provided in the Geonics manual. Of course, if the earth is not homogeneous, calculating σ from Eq. 2.6 will only provide an average value of conductivity over the depth of exploration for the EM31.

Other than the value for quadrature which provides an expression to compute the conductivity, the EM31 measures the in-phase component X as well. These in-phase data are more useful for locating finite buried metal (McNeill, 1980) and therefore not so useful in our investigation of mapping apparent conductivities.

In summary, each process of induction (receiver from transmitter, subsurface conductor from transmitter, and receiver from subsurface conductor) adds in a complex way to produce the final expression for the ratio of secondary to primary signals over a layered earth.

Overall, a body with high electrical conductivity produces strong electromagnetic fields which can be distinguished from the primary field, thus allowing the body to be located. Some rock bodies containing minerals that are themselves insulators may produce secondary electromagnetic fields, although not generally strong, if sufficient quantities of a conductive substance are also present (Kearey and Brooks, 1991). It therefore follows that if fractures in an insulating rock body (e.g. gneiss) are filled with conductive materials such as clays, leachate, or brines, then it may be possible to locate these materials, and therefore map the position of the rock fractures.

Conduction is largely electrolytic in near-surface rocks, taking place in connected pore spaces, along grain boundaries, and in fractures. The ions which conduct the current result from the dissociation of salts when dissolved in water. The more ions present, the greater the amount of charge carried. Therefore, solutions with a greater concentration of ions will be more conductive. Since brines and leachate contain high proportions of dissolved ions compared to fresh water, they will be conductive. It then follows that an insulating rock which is highly fractured will produce electromagnetic anomalies if the fractures are filled with a conductive substance such as brines or leachate (Ward, 1990).

Unlike many other minerals, clay particles are also conductive. Clay minerals are abnormally conductive because of their large ion-exchange capacity. Since some cations are adsorbed, there are too many ions present to produce one single layer of ions. This

double layer (Fig. 2.3) consists of a fixed layer immediately surrounding the clay particle and a diffuse layer which drops off in charge density exponentially with distance from the fixed layer. The ions in the diffuse layer, in contrast to the fixed layer, are free to move under the influence of an applied electric field. This layer then adds to the normal ion concentration and therefore increases conductivity (Ward, 1990). Similar to leachate and brines, the presence of clays within a fracture may also produce an anomalous secondary EM field when using EM methods. Most clays are hydrous aluminum silicates which form by weathering or hydrothermal alteration of aluminum and magnesium silicates, particularly feldspar and pyroxene, respectively (Klein and Hurlbut, 1993).

It should be noted that fracture walls are not always conductive. For example, Slater et al. (1998) found fractures mapped in southern Maine were more resistive than the surrounding bedrock. In some cases there will be no conductivity difference between the fracture and the surrounding bedrock. However, if the bedrock fractures in our area of study tend to be conductive due to either the presence of leachate flowing through them, the clays lining their walls, or the combination of the two, they may be detected.

2.3 Electromagnetic Azimuthal Methods

An EM system, such as the EM31, can therefore be used to locate fractures and their orientations when they are conductive. As an alternative to traditional profiling and contouring of EM data, azimuthal conductivity measurements using either the vertical- or horizontal-dipole orientation can be carried out. Data for azimuthal conductivity are collected at a fixed position by rotating the line joining the transmitter and receiver coils about a vertical axis and measuring the conductivity at equal angular intervals. The

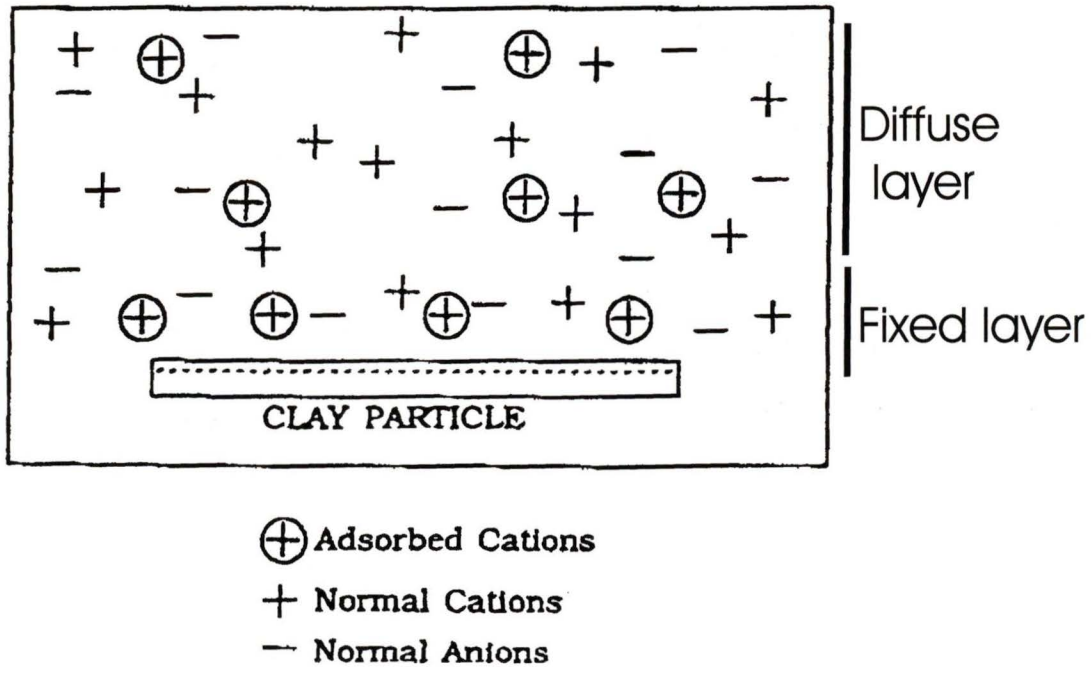

Figure 2.3. Clay particle with a fixed and a diffuse layer of ions (Ward, 1990).

objective is to map the directions of maximum (minimum) conductivity and relate these to electrical anisotropy (Taylor and Flemming, 1988). The direction of fractures in the underlying bedrock can be determined by correlating them with the directions of maximum (and sometimes minimum) conductivity. For the EM31, EM waves propagate as a dipole field and the eddy currents from the conductor usually produce a dipole or large loop field. Therefore the position of the transmitter, receiver, and the conductor and the coupling between all three determines the amount of anisotropy and/or heterogeneity.

Unfortunately, azimuthal EM surveying can be quite noisy as it is extremely difficult to keep the coils at correct angular increments. The signal-to-noise ratio can be increased in several ways. One approach is to design a filter based on the azimuthal amplitude spectrum (Slater et al., 1998). A simpler approach is to use the reciprocity theorem that states the EM measurement must be the same when the transmitter and receiver are interchanged. In other words, the measured conductivity at 0° is equal to the measured conductivity at 180°, the measured conductivity at 15° is equal to the measured conductivity at 195°, etc. Therefore, averaging conductivity values measured 180° apart can eliminate some of the noise due to factors mentioned above. Measurements can be made through two complete rotations (from 0 to 360° and from 360 to 720°) to suppress noise even further.

Most previous studies using EM azimuthal surveys (Sandberg and Jagel, 1996; Sandberg et al., 1996) obtain results with a symmetric configuration (i.e. rotating the instrument about a point of rotation located midway between the transmitter and receiver coils). However, asymmetric arrays have been used to improve sensitivity to anisotropy and to assist detection of subsurface heterogeneity (Bolshakov et al., 1995; Bolshakov et

al., 1997; Pervago et al., 1997) where the point of rotation moves in a systematic pattern, i.e. the mid-point between the transmitter and receiver moves a small distance relative to the transmitter-receiver separation (Slater et al., 1998).

With the symmetrical array, the reciprocity theorem states that interchanging transmitter and receiver should not alter the measurement value, i.e., the data set should be symmetric about 180°. With the asymmetric array, the presence of subsurface heterogeneity can result in non-180° symmetry (Bolshakov et al., 1997) because the mid-point has moved. If the subsurface is purely anisotropic, 180° symmetry will still be present with this type of array since conductivity anisotropy depends on array orientation alone. Heterogeneity, on the other hand, depends on both orientation and position. Therefore, the change in the mid-point of the transmitter–receiver for an asymmetrical configuration allows the system to distinguish between anisotropy and heterogeneity in the subsurface (Slater et al., 1998).

However, azimuthal surveys completed at Hartland Landfill were only completed using a symmetric configuration, rotating the EM31 about a single midpoint. This configuration worked in this instance since we were trying to determine orientations of preferred directions of groundwater flow which should relate to (at least at our scale of investigation) to the electrical anisotropy. We were interested in local anisotropy (or fracturing at each station) rather than overall heterogeneity of the area. Therefore, at the scale of sampling using the EM31 (perhaps an elliptical volume 6m deep x 3m wide x 5m long), the symmetrical configuration was considered sufficient for locating "local" anisotropy associated with fractures. Also, the azimuthal survey was carried out after the

traditional survey. The results of the traditional survey (Figs. 3.2, 3.3, and 3.6) indicate there are no large heterogeneous features present in the survey area.

2.4 Ground-Penetrating Radar

Ground-penetrating radar (GPR) is a technique for imaging shallow soil and rock structure with high resolution. In some ways, it is similar to both seismic and EM methods. It is similar to shallow seismic reflection in that it uses the reflection of electromagnetic energy (changes in dielectric constant versus the effects of acoustic energy caused by changes in density and elastic moduli for seismic methods). It is similar to EM in that EM diffusion and the propagation of radar waves through a medium are controlled by the electrical conductivity of that medium (Kearey and Brooks, 1991).

In GPR, a short radar pulse of electromagnetic energy is introduced into the ground in the frequency band of 10-1000 MHz. The propagation of EM waves at these frequencies is mainly controlled by the dielectric properties of the rock material, i.e., its ability to be polarized. Radar propagation velocity (V) is related to the dielectric constant by:

$$V = c/\sqrt{(\mu_r K)} \qquad (2.7)$$

where K is the dielectric constant (the ratio of the dielectric permittivity ε of the medium to that of free space ε_o where $\varepsilon_o = 8.854 \times 10^{-12}$ F/m), μ_r is the relative magnetic permeability of the medium (i.e. , $\mu_r = \mu/\mu_o$ where $\mu_o = 4\pi \times 10^{-7}$ H/m is the magnetic

permittivity of free space), and $c = 1/\sqrt{(\mu_o \varepsilon_o)} = 3 \times 10^8$ m/s (0.3 m/ns) is the velocity of EM waves in free space (Telford et al., 1995).

Since μ_r is approximately equal to unity for many rock materials (Sharma, 1997), radar velocity is mainly controlled by K, the dielectric constant of the medium. Table 2.1 lists dielectric constants and propagation velocities of radar waves in various materials. The water content of materials exerts a strong influence on the propagation of a radar pulse since the dielectric constant of water is approximately 80 while most geological materials range from 3-10 (Sharma, 1997).

Contrasts in the conductivity and dielectric properties across an interface cause part of an impinging radar pulse to be reflected. The result of such contrasts includes a reduction in the amplitude of the radar pulse at the reflecting boundary depending on the contrast and thickness of the layer. Although fractures may not be large in size, they can produce strong radar reflections because they serve as active seepage conduits for fluids with high dielectric constants or because they contain clay and other weathering products which may act as subsurface reflectors if they are of low attenuation.

GPR is most typically used as a method for localized high resolution mapping. The range of penetration of a radar pulse will decrease with increasing conductivity. Therefore, under ideal conditions of low conductivity ($<10^{-2}$ S/m), penetration depth can reach 50 m, whereas in areas of high conductivity ($>10^{-2}$ S/m), penetration may only reach as far as 2 m. Most commonly, a penetration depth of 20 m is reached on average (Sharma, 1997). Since our area is generally of low background conductivity with little overburden, GPR can aid in fracture detection, especially when combined with EM and geological data sets.

Table 2.1. Dielectric constant, K, and propagation velocity, V, of radar waves in some geological materials and contaminant fluids (Sharma, 1997).

Material	K	V (m/ns)
Dry sand/gravel	4-10	0.15-0.09
Wet sand/gravel	10-20	0.09-0.07
Dry clay/silt	3-6	0.17-0.12
Wet clay/silt	7-40	0.11-0.05
Cement (dry/wet)	6-11	0.12-0.09
Granite	4-9	0.15-0.10
Limestone	4-8	0.15-0.11
Dry salt	5-6	0.13-0.12
Permafrost	4-5	0.15-0.13
Glacier ice	3.5	0.16
Fresh water	81	0.03
Methyl alcohol	31	0.05
Petroleum/Kerosene	2.1	0.20
Aviation gasoline	1.95	0.21
Air	1	0.30

CHAPTER 3

Data Collection

3.1 Introduction

Three types of geophysical surveys were carried out for this thesis. These included an electromagnetic survey using a Geonics EM31-MK2 Terrain Conductivity meter, an azimuthal conductivity survey using the same instrument, and a ground-penetrating radar (GPR) survey using a Sensors and Software PulseEKKO 100 system.

In addition to these geophysical surveys, several geological methods were used to collect data. Hand samples of the bedrock were taken and subsequently thin-sectioned and examined petrographically. Alteration products in some fractures were removed and sieved to determine clay content. The orientations of these and other fractures in exposed outcrops were recorded and plotted. As well, geochemical data collected by the Hartland Landfill Monitoring Program were analyzed.

3.2 EM Data

3.2.1 Profiles and Contouring

The EM31 survey was carried out in August of 1999 to measure and record terrain conductivity measurements (apparent conductivities) along E-W survey lines. The depth of penetration is expected to be nearly 6 m. Since the volcanic bedrock in the area is highly resistive, anomalous conductivity highs may be the result of fractures which are filled with contaminated groundwater or with alteration products such as clays.

The EM31 survey in the east-west direction had a line spacing of 10 m and covered an area approximately 195 x 240 m (Fig. 3.1). Vertical-dipole readings were taken along all lines at 2 m intervals with the instrument oriented parallel to the direction of travel (E-W) at waist height. Readings were then stored in a solid state memory data logger and subsequently downloaded into a spreadsheet program. Along north-south Lines 20 W to 60 W and along east-west Lines 50 N to 10 S and Line 110 S, horizontal-dipole measurements were also taken. The complete dataset can be found in the disc at the back of this thesis.

The EM survey lines extended from 55 m N to 140 m S (Fig. 3.1). Each tick on these survey lines represents a station where EM31 vertical-dipole measurements were taken. Gaps on survey lines where no measurements were recorded was due to localized debris and/or inaccessibility. Survey lines from 40 N to 55 N were completed every 5 m instead of the usual 10 m since this locale is closest to the base of the landfill.

The eastern portion of the area was covered with dense brush and was only surveyed in patches where line cutting was not required. Environmental considerations limited access to those lines where the brush could be traversed. The edge of the Phase 1 landfill is approximately 100 m north of the northern boundary of the contour map. Several large metal bins about 30 m north of the north boundary caused so much cultural interference that data north of line 30 N is subject to scrutiny.

The contoured conductivity values for the east-west vertical-dipole lines to the west are presented in Figure 3.2 (see Appendix A for a complete contour map of the area). Some obvious conductivity trends are visible on this map. Conductivity values are

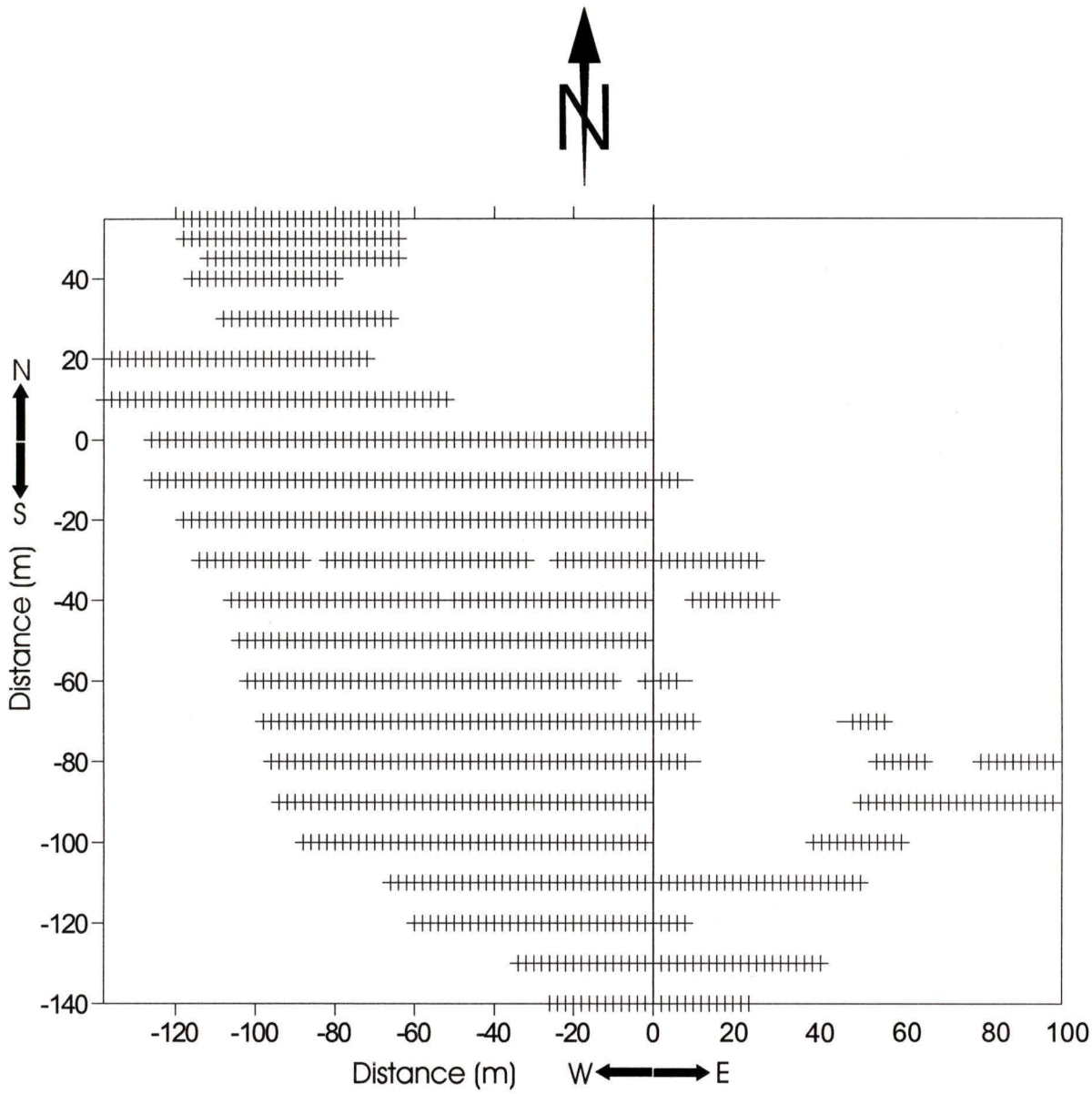

Figure 3.1. Each tick represents a station where EM measurements were taken. Box to the left shows data which is contoured in Fig. 3.2. A contour map of the full area is given in Appendix A. Map location can be determined from monitor well location 19 (see disc at back of thesis for its northing and easting coordinates) which lies on Line 110 S at 48 E.

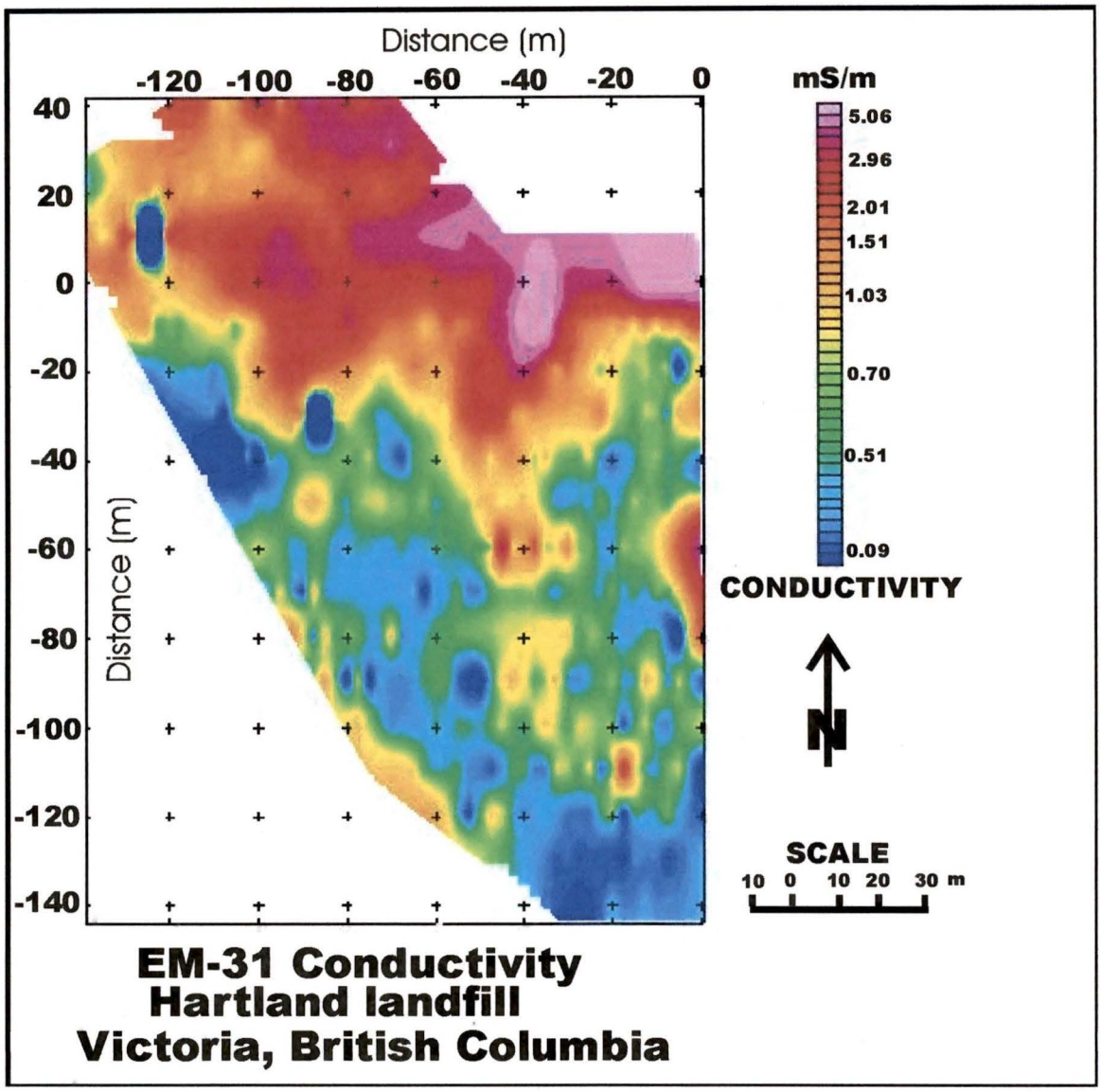

Figure 3.2. Contour map indicating apparent conductivities in mS/m. Prominent features include higher conductivities closer to the landfill, located approximately 50 m north of the mapped area, and conductivities approaching background levels farther to the south and away from the landfill. Linear conductive highs are obvious near 40 W and 85 W and other less prominent linear features are also present.

generally higher closer to the landfill in the north, and lower farther from the landfill in the south. In fact, conductivity measurements appear to reach background levels in the southern portion of the survey. There are also some obvious N-S trending conductivity highs, the most pronounced of which is located at approximately 40 m W.

A stacked profile (Fig. 3.3) for Lines 0 S to 100 S clearly shows the two areas with prominent conductive highs near 40 W and 85 W. These highs are more pronounced on Lines 0 S to 60 S. From Lines 70 S to 100 S conductivity measurements return to background levels.

Line 20 S was surveyed twice to observe and analyze repeatability and consistency of the EM data collection. The two surveys clearly agree very well (Fig 3.4). The root-mean-square (rms) difference in conductivity between the profiles is 0.41 mS/m which provides a quantitative estimate of the conductivity measurement error. Most of this variance can be attributed to instrument drift, errors in location of the two surveys which were carried out at different times, and human error.

Another way to gauge repeatability and error was to survey along lines perpendicular to the east-west profiles (Fig.3.5). These north-south profiles were completed along lines 20 W to 60W (Fig. 3.6). The profile along 40W, which closely follows the axis of the easternmost linear conductor, clearly shows the increase in conductivity when going from south to north. The difference in measurements in the north-south and east-west directions at the same station indicate that the direction of measurement influences the conductivity observed (Table 3.1). This will account for the higher rms value of 0.77 mS/m for this dataset since the instrument at each common station was oriented at right angles to one another. This value was calculated from the

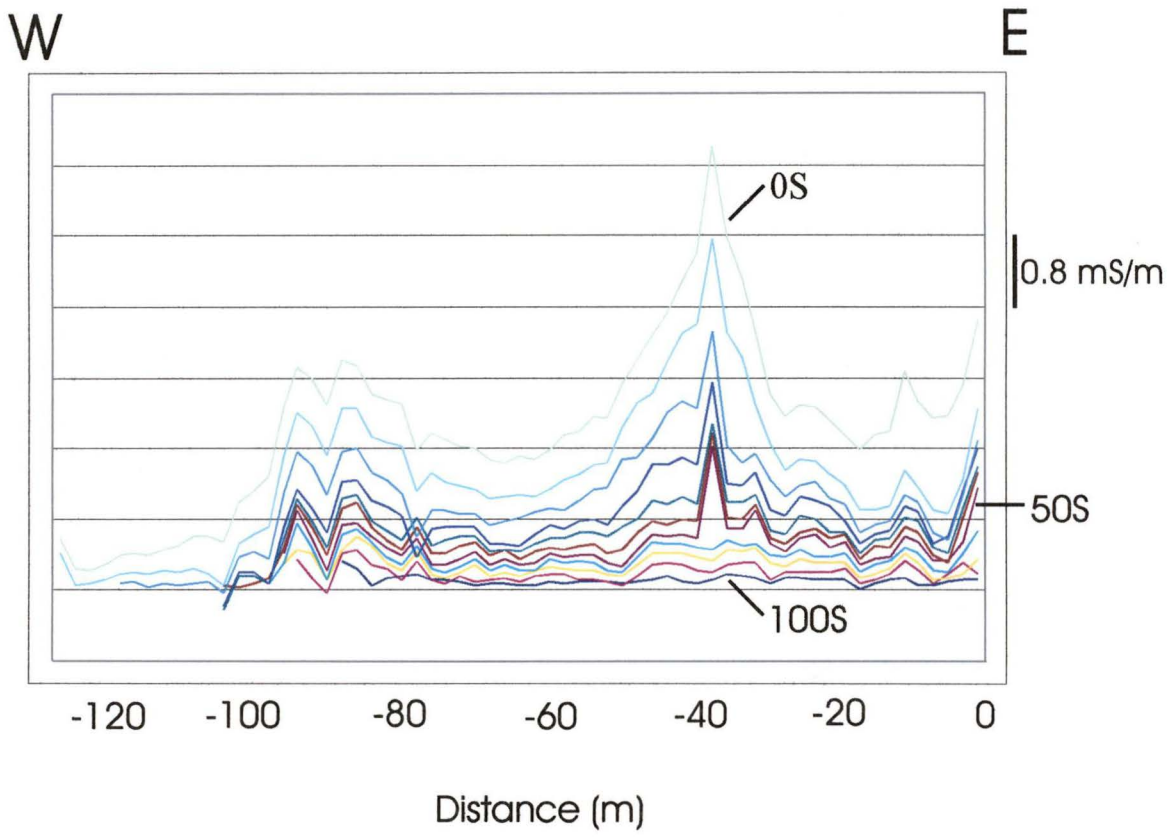

Figure 3.3. Stacked profile of apparent conductivities from Line 0 S to Line 100 S, every 10 m. Obvious features are (1) higher conductivites closer to the landfill (0 S) and (2) low conductivities nearing background levels occur farther from the landfill (100 S) and (3) linear conductive highs concentrated around 40 W and 85 W. Each profile is offset from the neighbouring one, and therefore, there is no zero reference point.

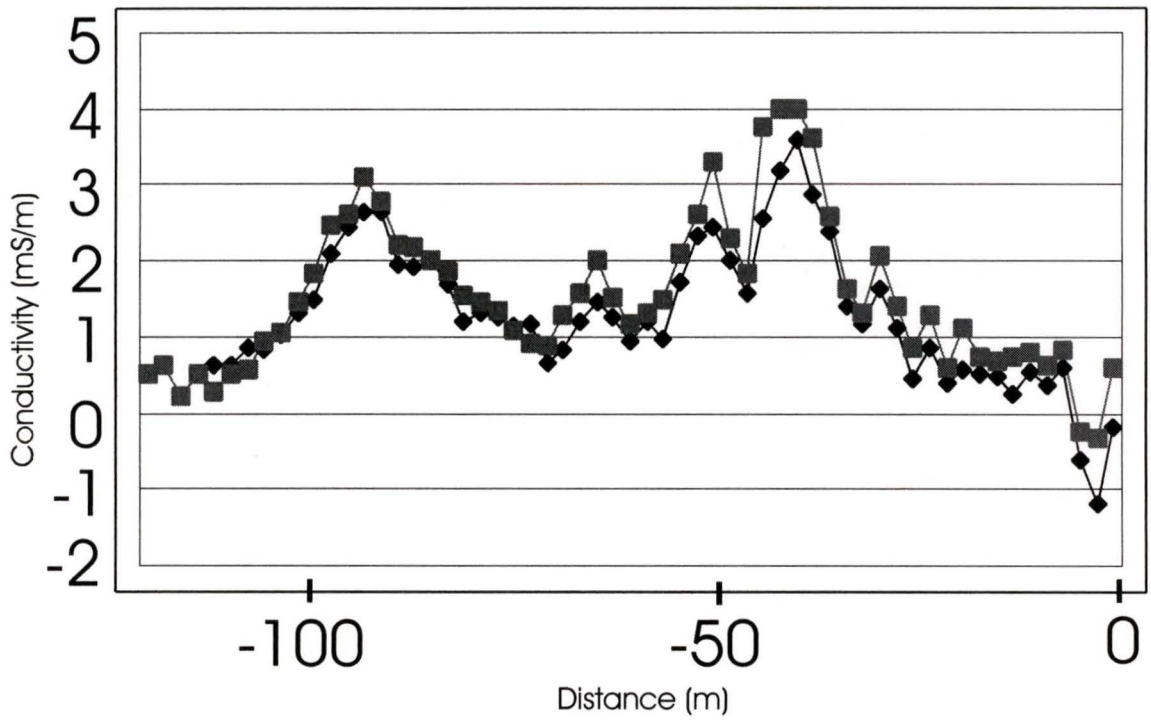

Figure 3.4. Conductivity measurements were measured twice along Line 20 S. The two sets of values agreed well, with an rms conductivity difference of 0.41 mS/m. This difference is mostly due to positioning differences between the two surveys which were completed on two different days.

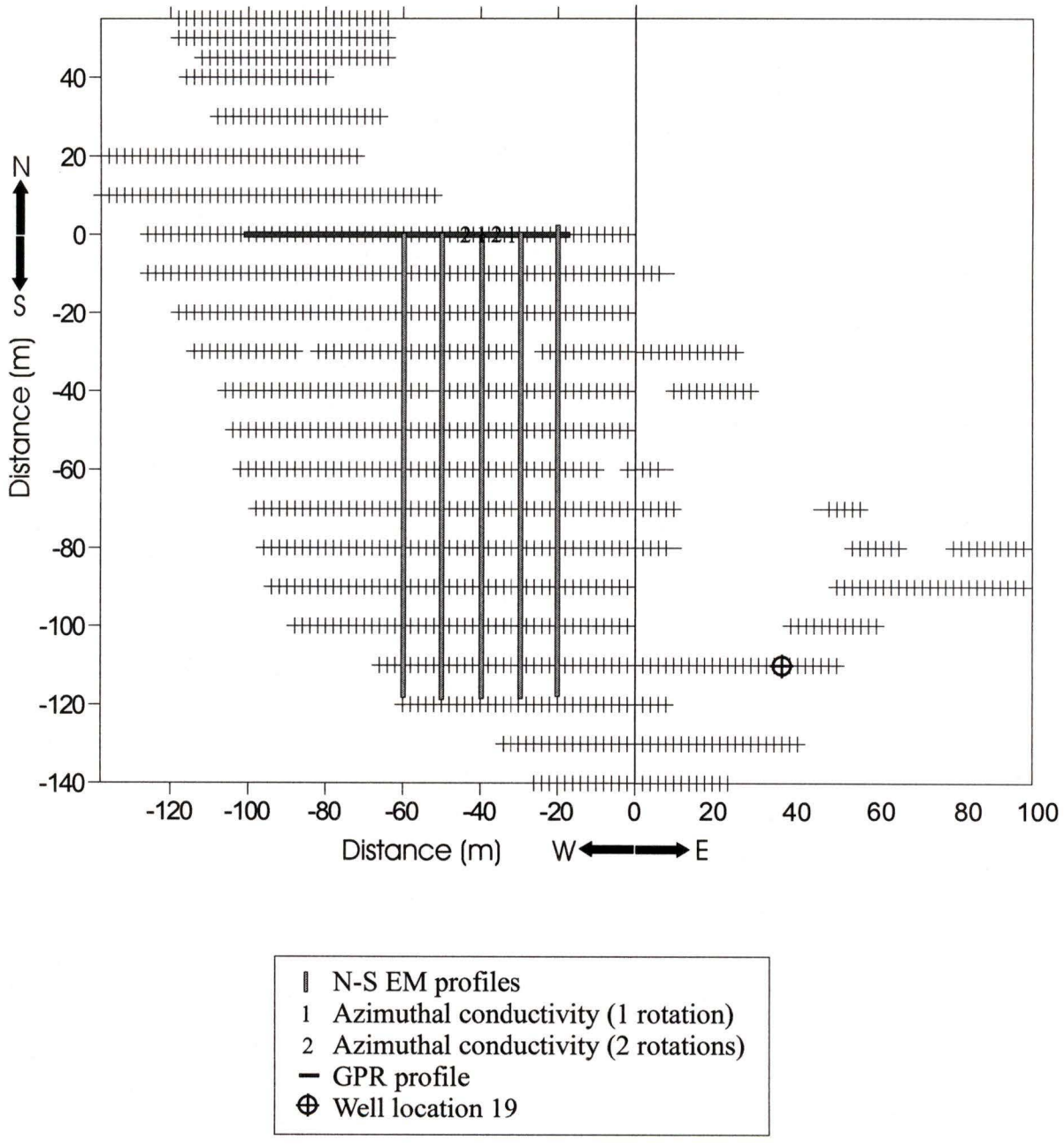

Figure 3.5. Each tick represents a station where EM measurements were taken. The positions of the N-S EM profiles (Fig. 3.6), EM azimuthal plots (Figs. 3.7 and 3.8) GPR profile (Fig. 3.9), and well 19 (Fig. 4.2) are shown.

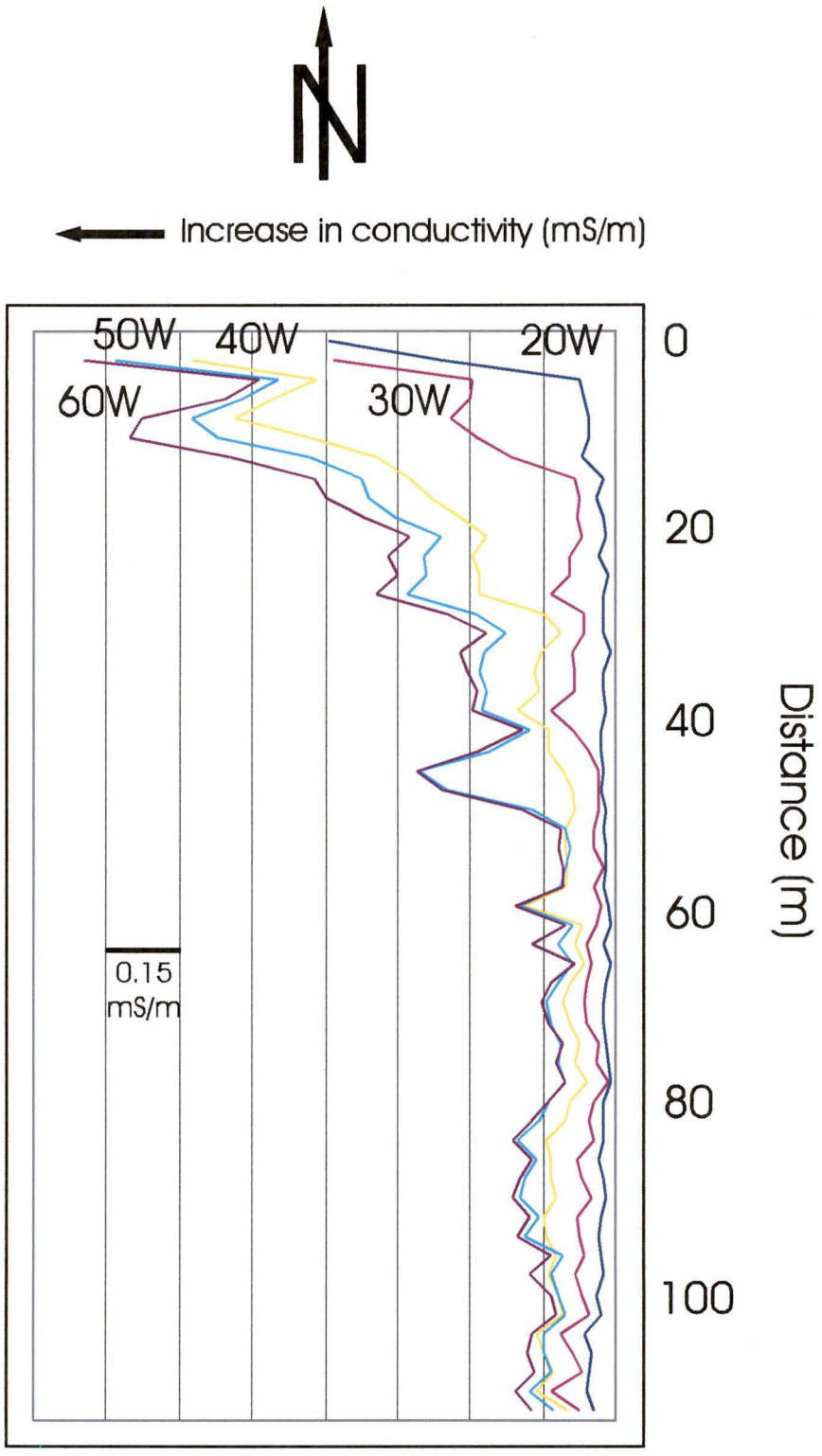

Figure 3.6. Conductivities along N-S lines 20 W to 60 W. Each profile is offset from the neighbouring one, and therefore, there is no zero reference point.

Table 3.1. Conductivity measurements taken at the same station in north-south and east-west directions and their observed differences.

Position (E-W)	Position (N-S)	North-south line conductivities (mS/m)	East-west line conductivities (mS/m)	Difference between N-S and E-W conductivities (mS/m)
-20	-100	0.875	0.725	0.15
-20	-90	0.475	0.75	-0.275
-20	-80	0.325	0.475	-0.15
-20	-70	0.25	0.675	-0.425
-20	-60	0.3	0.3	0
-20	-50	0.275	0.45	-0.175
-20	-40	0.4	0.2	0.2
-20	-30	0.15	0.825	-0.675
-20	-20	0.475	1.1	-0.625
-20	-10	0.9	1.3	-0.4
-20	0	4.8	3.675	1.125
-30	-100	0.625	0.475	0.15
-30	-90	0.5	0.3	0.2
-30	-80	0.25	1.075	-0.825
-30	-70	0.2	0.55	-0.35
-30	-60	0.5	1.625	-1.125
-30	-50	0.325	0.4	-0.075
-30	-40	0.35	0.625	-0.275
-30	-30	1.025	No value recorded	---
-30	-20	0.75	2.05	-1.3
-30	-10	2	2.575	-0.575
-30	0	2.95	3.625	-0.675
-40	-100	0.7	0.425	0.275
-40	-90	0.95	0.975	-0.025
-40	-80	1.35	0.85	0.5
-40	-70	0.525	0.7	-0.175
-40	-60	0.35	1.25	-0.9
-40	-50	0.775	1.1	-0.325
-40	-40	1.125	1.225	-0.1
-40	-30	0.875	1.25	-0.375
-40	-20	2.75	4	-1.25
-40	-10	3.7	5.9	-2.2
-40	0	3.9	5.15	-1.25
-50	-100	-0.224	0.45	-0.674
-50	-90	0.55	-0.175	0.725
-50	-80	0.8	0.7	0.1
-50	-70	0.55	0.275	0.275
-50	-60	0.4	0.55	-0.15
-50	-50	-0.125	1.125	-1.25
-50	-40	1.625	1.625	0
-50	-30	1.55	2.8	-1.25
-50	-20	1.3	3.3	-2
-50	-10	1.85	2.225	-0.375
-50	0	2.125	3.125	-1
-60	-100	0.3	0.525	-0.225
-60	-90	0.2	0.575	-0.375
-60	-80	0.125	0.6	-0.475
-60	-70	-0.05	0.475	-0.525
-60	-60	0.725	0.5	0.225
-60	-50	0.3	0.425	-0.125
-60	-40	0.3	0.7	-0.4
-60	-30	0.65	0.975	-0.325
-60	-20	0.95	1.175	-0.225
-60	-10	2.15	1.3	0.85
-60	0	0.875	2.9	-2.025

differences in values of conductivities between north-south and east-west measurements at all crossover points.

3.2.2 Azimuthal Data

Azimuthal conductivity measurements using the vertical-dipole orientation were carried out at 4 m intervals along several of the E-W lines. Data for azimuthal conductivity were collected by rotating the line joining the transmitter and receiver coils about a vertical axis and measuring the conductivity at equal angular intervals of 15°. To compare, raw data (top) at stations 32 W and 40W are presented with data (below) which have been averaged using the theory of reciprocity (as detailed in Chapter 2; Fig. 3.7). Since receiver and transmitter can be interchanged, values at 0 and 180° or 15 and 195° etc. should be the same. Therefore, the averaging of the two will reduce noise in this data set.

To further investigate noise, at some stations, measurements were made through two complete rotations (from 0 to 360° and from 360 to 720°). For example, along line 0 S, at 36 W and 44 W (Fig. 3.8), noise was reduced by averaging the same data points on each rotation (e.g. averaging both 15° measurements together).

In both instances, whether it be averaging one or two rotations, (Figs. 3.7 and 3.8), the data are quite repeatable, although there is some noise present. Note that the noise is reduced and the direction of maximum (and minimum) is clearer after averaging. Conductivity variations of 15 to 30% between maximum and minimum values are not uncommon in this data set. The values of conductivity are also consistent with values on

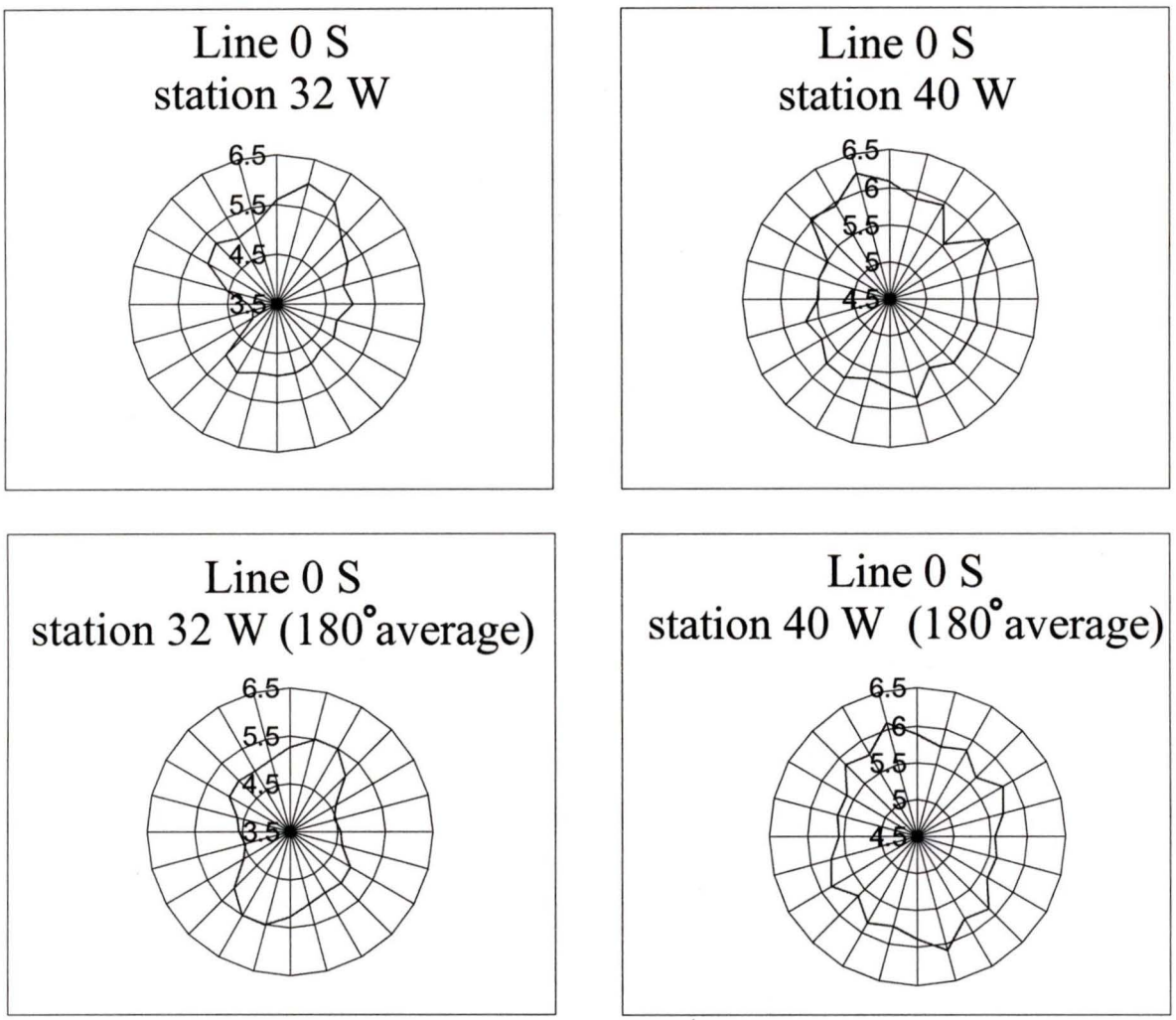

Figure 3.7. Comparison of azimuthal conductivities (mS/m) at stations 32 W and 40 W on Line 0 S before and after averaging data 180 degrees apart. Note the decrease in noise and the sharper definition of maximum and minimum conductivity values.

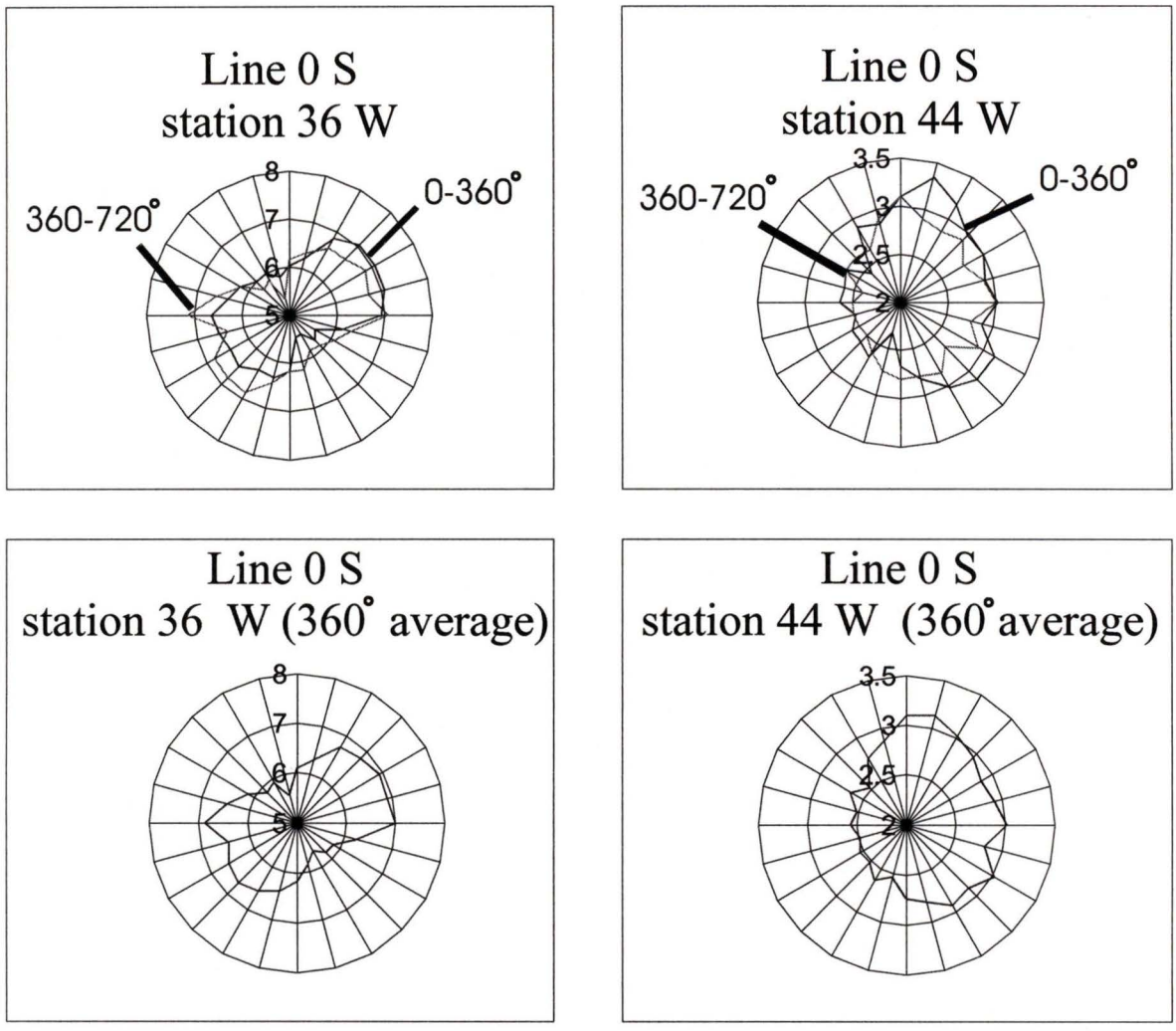

Figure 3.8. Comparison of azimuthal conductivities (mS/m) at stations 36 W and 44 W on Line 0 S before and after averaging of two complete rotations. Note the decrease in noise and the sharper definition of maximum and minimum conductivity values.

the east-west lines and, for that matter, on the north-south lines as well. Other examples of this repeatability are shown in Appendix B.

3.3 GPR Data

Ground-penetrating radar (GPR) offers a high resolution sounding capability with detection of features a few centimeters in thickness down to depths of several meters. The radar system uses a short pulse of high frequency (100 MHz in this case) electromagnetic energy which is transmitted into the ground. The propagation of the radar signal depends on the high frequency electrical properties of the ground. The electrical properties of the geological materials are primarily controlled by water content. Therefore, radar reflections seen in the bedrock are most likely caused by fluid filled fractures (Davis and Annan, 1989). In our case, reflections are most likely due to bedrock fractures filled with hydrous clays or conductive groundwater.

A Sensors and Software PulseEKKO 100 was used to perform the GPR survey. GPR profiles were conducted along pre-existing EM survey lines where variations in conductivity were noted (Fig.3.5). Antennae were separated by 1 m and oriented perpendicular to the line direction (i.e. north-south) and the step size along the lines was 0.5 m. The only processing applied to the GPR profiles was a trace-to-trace averaging plus an automatic gain control with a window width of 10 ns.

A GPR profile (Fig. 3.9) along east-west conductivity line 0 S is compared with the EM conductivity of one of the largest conductivity anomalies. Some continuous reflectivity can be identified down to a depth of 5 m (assuming a velocity of 0.1 m/ns which is a reasonable average velocity). In the near-surface, from about 0 to 2 m, a band

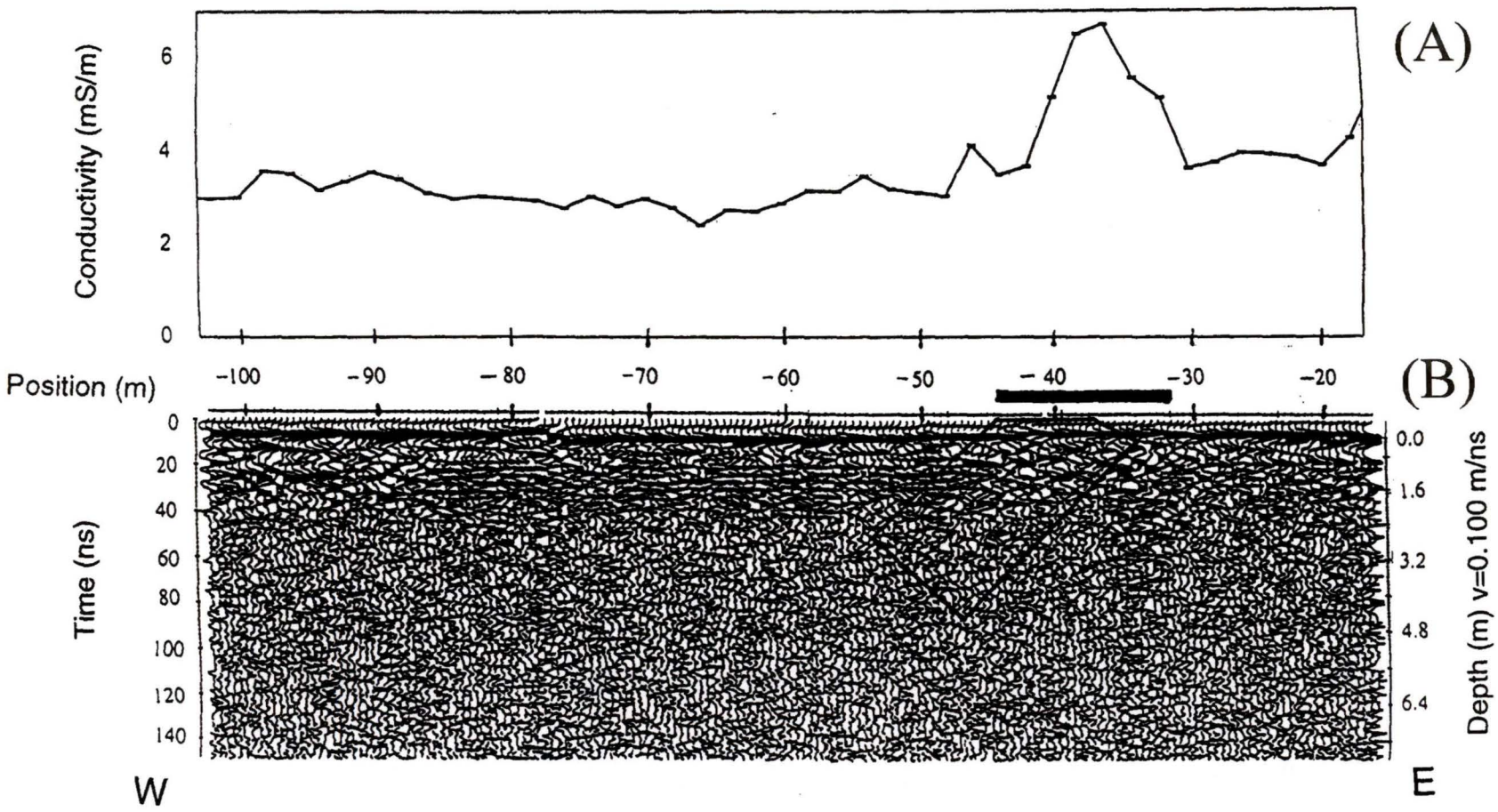

Figure 3.9. EM (A) and GPR profile (B) of line 0 S from -103 (103 W) to -17 m. The solid bar from -45 to -32 m shows the region where shallow reflectors (0 to 2 m depth) are disrupted. This disruption shows the presence of what may be a set of fractures. This region coincides closely with the conductivity high near 40 W.

of continuous high-amplitude reflectors is disrupted over the region from approximately 32 to 45 W. This same region, as shown on the EM profile above, indicates the position of a conductivity high (6 mS/m versus 3 mS/m). All GPR data collected, some of which show similar discontinuities, can be seen in Appendix C.

3.4 Geological Data

Hard rock samples of the ubiquitous gneiss throughout the area were collected and examined petrographically. In general, the fine-grained to medium-grained gneiss is composed mainly of hornblende (~60-65%) with nearly equal amounts of plagioclase and quartz (~40-35%). Accessory minerals include muscovite, biotite, calcite, titanite, apatite, and opaque minerals. Sericite and sausserite alteration is intense with moderate amounts of chloritization and low amounts of hematite. Styolites and veins are present in all samples and mainly filled with quartz and muscovite.

A representative sediment sample was taken from a fracture located on the westernmost Phase 2 rockface. The sample was placed into a sieve to determine the clay content of the material within the bedrock fractures. By weight, sieve analyses indicated that 4.8% of the material was clay sized (<1/256 cm).

Fracture orientations were recorded at two different rockfaces bordering the Phase 2 landfill (30 measurements at each locale). The first was located at the same rockface mentioned above and the second location was located just outside of the landfill property, north of the leachate lagoon. The dominant fracture directions at Hartland landfill strike approximately NE-SW, SE-NW, and N-S (Fig. 3.10).

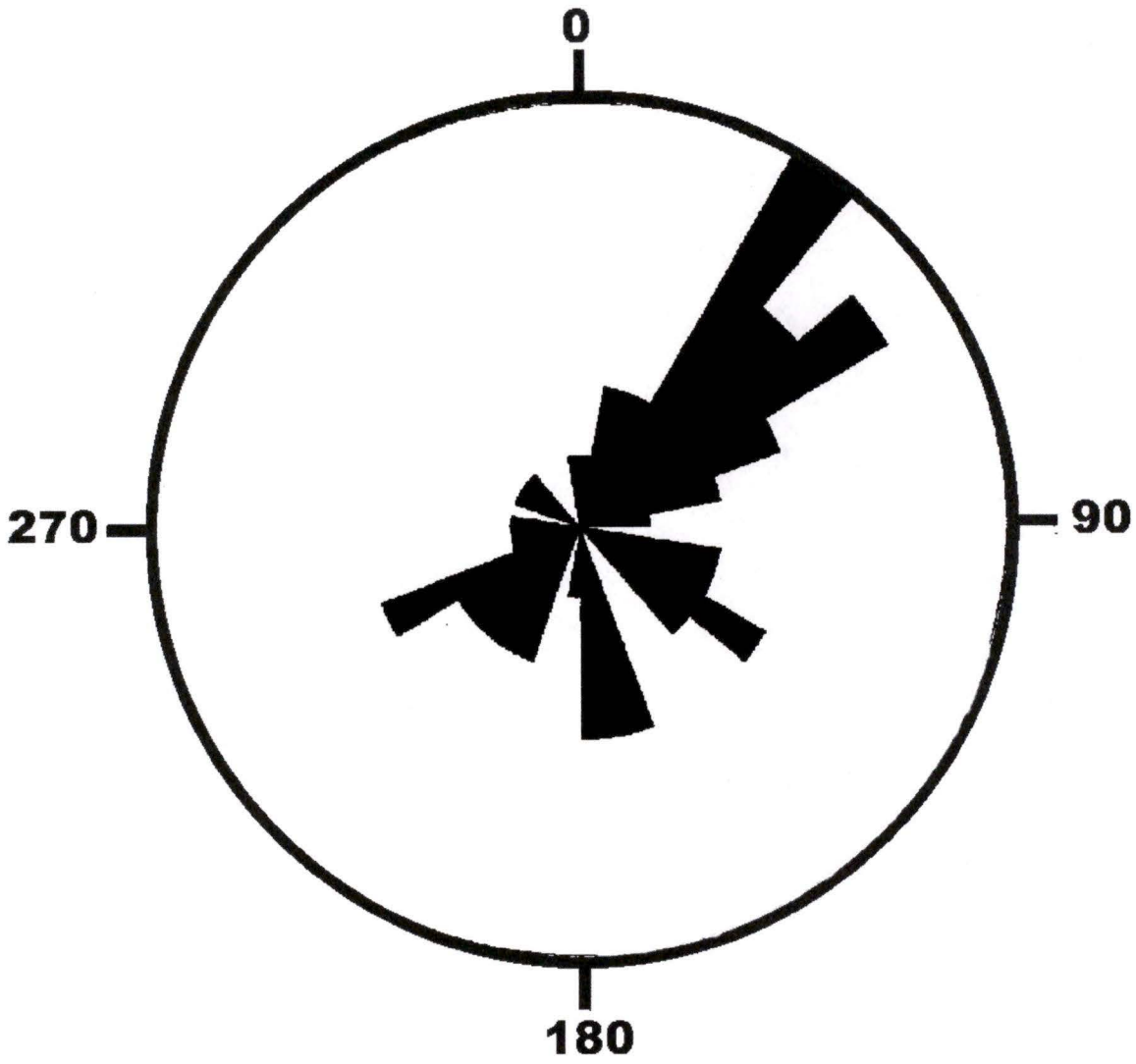

Figure 3.10. Rosette diagram indicating that the main fracture directions in outcrops strike approximately NE-SW, SE-NW, and N-S.

In 1997, a quarry plan was completed for Hartland Landfill to provide a comprehensive plan for rock quarry development at the landfill. During the survey, over 80 fractures were measured. Most of the fractures were steeply dipping and clustered to the NE-SW, NW-SE, and E-W (Sperling Hansen, 1997), not unlike the main fracture directions found in this study.

CHAPTER 4

Interpretation and Discussion

4.1 Introduction

A major goal of this study was to determine if there is a relationship of bedrock fracturing to electrical conductivity and anisotropy. Electromagnetic methods were used to map conductivity patterns, with linear geophysical anomalies indicating the presence and orientations of subsurface bedrock fracturing. Orientation of individual fractures was also detected by measuring conductivity at a given location over a range of azimuthal angles. These data were interpreted with ground-penetrating radar profiles and with field geological measurements.

4.2 Electromagnetic Methods

There are several features that stand out on the EM contour map (Fig. 3.2). The conductivity in the northern portion of the map is significantly higher than in the southern portion, indicating a subtle leachate front is propagating from the landfill towards the south. The background conductivity values in the northern portion of the map are typically 4 mS/m or greater while the background conductivity in the southern portion is between 0.5 and 1 mS/m. The higher conductivity region continues southward to approximately 60 S before returning to background levels. This is an indication that the leachate front has only travelled this far. It should be noted that these changes in

conductivity are very subtle and the leachate is not very conductive when compared to background levels. However, since there is very little overburden in the area, conductivity changes are most likely associated with the presence of leachate and not due to changes in overburden thickness. It is also possible that conductivity highs are caused by the presence of clays lining fracture walls. Since the EM31 system is unable to distinguish between the two, conductivity highs may be a result of either leachate and/or clays.

In addition, there are two approximately linear north-south conductors, one near station 40 W with a width between 10 and 15 m, and one near station 85 W with a width between 12 and 25 m. These linear zones are thought to be fracture systems containing leachate and/or clays. The conductivity of these zones is higher than the surrounding bedrock and approaches values between 1.0 and 1.5 mS/m south of line 60 S. These strong, narrow conductive features are also easy to recognize on the east-west stacked profiles in Figure 3.3.

The contour map (Fig. 3.2) indicates that many conductivity trends form a nearly N-S linear pattern. Since the data were collected in an E-W direction, these trends are robust features of the data and are definitely not an artifact of the collection direction. These obvious N-S conductivity trends may be indicative of a leachate front flowing through fractured bedrock in this direction.

In contrast with the contoured conductivity trends, the azimuths of maximum conductivity are not strictly N-S (as it is in Fig. 3.2), even when averaging is completed to reduce noise (Fig 4.1). The angle of the maximum conductivity tends to change direction at different stations along a line and has an average azimuth of $11° \pm 51°$

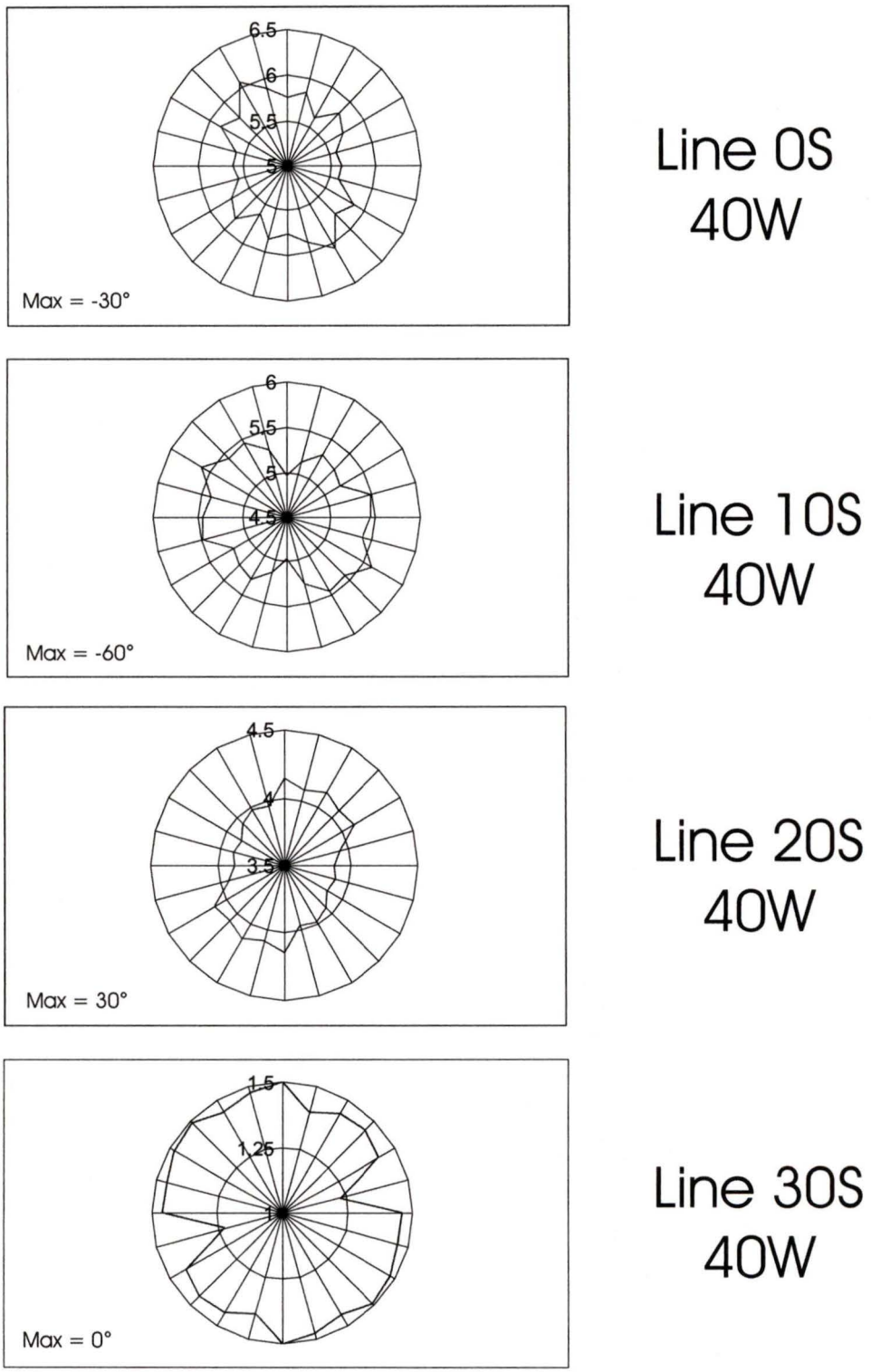

Figure 4.1. EM Azimuthal plots of apparent conductivities (mS/m) for Lines 0S to 30S at 40W, aligned approximately along the most prominent linear conductivity feature in Fig. 3.2. To reduce noise, points separated by 180 degrees were averaged. Average azimuth for direction of maximum conductivity is 11° ± 51°.

(calculated from first rotation of all sample locations). These changes from station to station and the large azimuth variance (± 51°), could be related to the fact that linear EM and azimuthal EM measurements were taken on different days with corresponding variations in instrument position and orientation, or due to local subsurface heterogeneities. More likely however, this variance is related to the small measurement scale of the EM31 system which is perhaps 5 m in the direction of the transmitter-receiver and 3 m perpendicular to this direction (McNeill, 1980). Consequently, going from station to station samples different portions of the ground and hence can map differently oriented fractures.

4.3 Ground-Penetrating Radar

An EM conductive high is present near and along 40 W from approximately 0 S to 60 S (Fig. 3.3). This feature is most prominent along Line 0 S (Fig. 3.9a). The boxed area on the GPR profile (Fig. 3.9b) outlines the region where continuous reflectors are disrupted and indicates the region where fractures may be present. The disrupted region aligns with the region of maximum conductivity determined from the EM data, which supports the interpretation that the high conductivity anomaly may be associated with flow along fractures, or at least with some type of conductive material within the fractures. The same is true for other GPR profiles south of line 0 S which also show discontinuous features that may be interpreted as fracture zones (Appendix C).

4.4 Geological Data

4.4.1 Mineralogy

The rock samples of the gneiss collected at Hartland Landfill provide evidence for the possible cause of anomalous conductivities in the area. The presence of styolites and veins present in all samples show that these rocks were stressed during metamorphism. It therefore follows that these stresses should also be seen on a larger scale, producing faults and fractures at depth, creating fractured bedrock and therefore potential conduits for contaminated groundwater flow. In addition, mineralogical components such as feldspar can alter into clay minerals (Klein and Hurlbut, 1993). Such altered products may be located in the fracture systems. These samples contain alteration products such as sericite, sausserite, chlorite, and hematite. Such intense alteration in several samples would indicate the likelihood of clay minerals being present at depth as well. Further evidence of this was found during sieve analysis where nearly 5% of sediment removed from exposed fractures was composed of clay. Given this evidence, conductive highs may be a result of clays along the walls of these fractures, leachate within the fractures, or a combination of both.

4.4.2 Fracture Detection in Outcrops

Fracture orientations were recorded at two different rockfaces at the landfill. The dominant fracture directions at Hartland landfill strike approximately NE-SW, NW-SE, and N-S (Fig. 3.10). The EM azimuthal data also shows conductive highs oriented in similar directions (azimuth average $11° \pm 51°$) as these known fracture directions in

outcrops (Figs. 3.7, 3.8, 4.1, and Appendix B). As well, these fracture orientations are consistent with the earlier work done by Sperling Hansen Associates Inc. (1997).

4.4.3 Geochemistry

As shown in section 1.2.4, the geochemical data collected at Hartland Landfill appears to suggest some form of leachate front may have entered the groundwater system. Concentrations of parameters which exceed acceptable guideline criteria (e.g. conductivity, chloride, ammonia, and iron) are concentrated near the landfill, and down gradient from the landfill, less and less evidence of contamination is obvious. However, it should be noted that geochemical analyses from year to year generally show that conditions are not worsening, but improving.

Monitoring well 19-1-1 is located on EM31 traverse line 110 S at 48 m E (Fig 4.2). The sharp peak on the EM plot is caused by the well casing which is metallic. It is therefore not possible to compare the EM apparent conductivities to the geochemical measurements at this location.

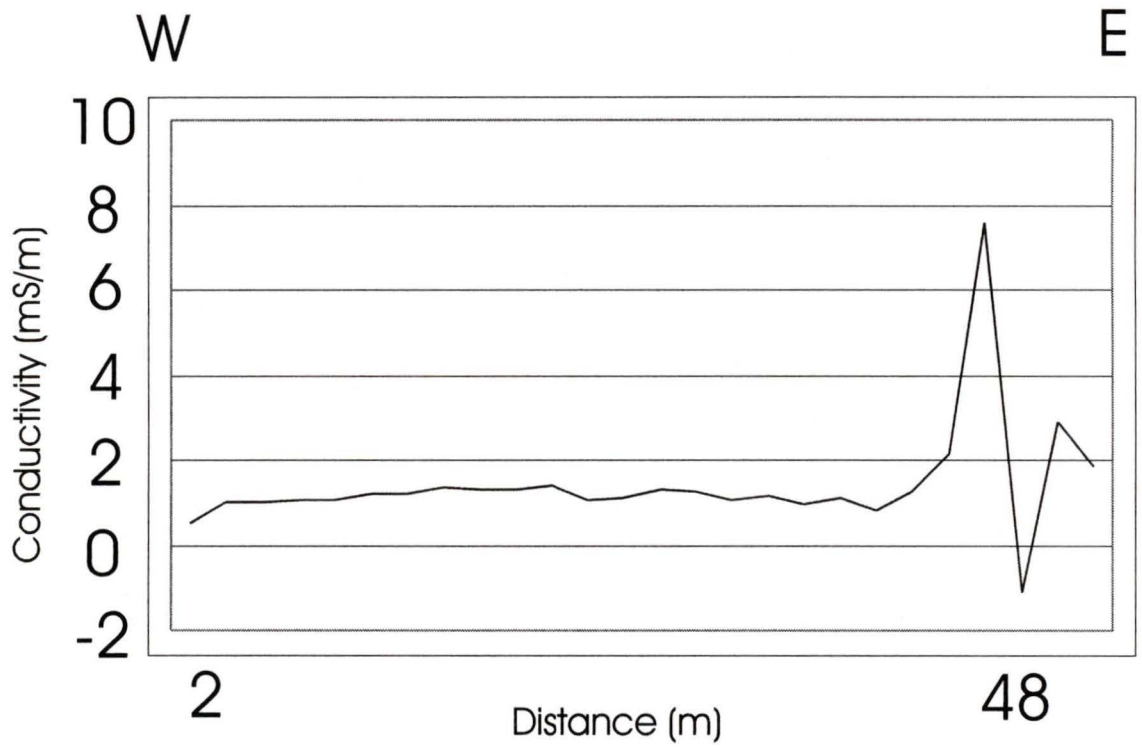

Figure 4.2. Plot of apparent conductivities on Line 110 S where two wells at location 19 intersect the EM profile line at 48 E. Note the negative values of conductivity which are typical of a finite, strong conductor response such as that caused by the metallic well casing (McNeill, 1980).

CHAPTER 5

Conclusions

Using the EM31-MK2 ground conductivity meter, several conductivity profiles were carried out down-gradient from the landfill, just south of the original Phase 1 footprint. Although a clay berm was constructed to direct most groundwater and leachate towards the leachate lagoon in the north, some southern flow of groundwater exists. Most likely, groundwater percolated vertically down-gradient in the Phase 1 landfill area and when it reached open bedrock fractures it started to move down-gradient within the bedrock, under the berm, and towards our area of study. Conductive highs (thought to be a leachate front) are apparent on the EM contour map as well as on EM stacked profiles, showing conductivity highs (4 mS/m) near the landfill and returning to background levels (1 mS/m) farther from the landfill. Other prominent features are the linear N-S conductivity trends which have been interpreted as more densely fractured bedrock and conduits for groundwater flow.

Using the same instrument, vertical-dipole EM azimuthal data was recorded at several locations along original EM profile lines. Using the theory of reciprocity, interchanging the transmitter and receiver should not affect the measurement, therefore, points 180° apart could be averaged to reduce noise. Some stations were even measured (at 15° intervals) through two complete rotations to further investigate noise. In addition, sources of error include human error and variance in instrument position and orientation.

However, these data still show that at most locations there is generally a preferred direction of conductivity maximum which can vary from the minimum by more than 30% and the orientation of maximum conductivity averages around $11° \pm 51°$. This electrical anisotropy has been interpreted as possibly being a result of fractured bedrock containing leachate and/or clays. When the EM31 is parallel to leachate- and/or clay-filled fractures, conductivity measurements are more pronounced.

Conductivity highs may represent fracture surfaces lined with clays, leachate-filled fractures, or the combination of the two. Since the geophysical methods used cannot distinguish between the two, further work is required. Possible methods may include using IP to determine the presence of clays as well as the installation of new monitoring wells along areas of high conductivity (40 W and 85 W) to confirm the presence of fractures and assess the groundwater quality in those areas. In time, data from these monitoring wells will tell if leachate is present and whether it is dissipating or worsening.

The ground-penetrating radar (GPR) data collected show fairly continuous features in the subsurface. However, there are sections where discontinuities are prevalent. These areas are concentrated where conductive highs are located (40 W) on EM profiles and on the contour map. The EM data suggests this to be an area of fractured bedrock containing leachate and/or clays, and the GPR discontinuities in the same area suggest fluid-or clay-filled fractures as well.

Geological sources of data were also used to complement the geophysical work. Petrographic analyses has shown that rock samples are highly fractured and altered. They contain mineralogy (20% feldspar) that can be altered to clays which would help in

fracture detection when using EM methods. As well, clays have been detected in bedrock fractures at the surface. In addition, fracture measurements taken from outcrops are oriented similar to the direction of conductivity highs on the EM conductivity map as well as EM azimuthal plots.

Geochemical analyses have shown throughout the years that leachate has entered the groundwater system and is travelling down-gradient from the landfill. However, very little evidence of leachate has been found in wells farthest from the landfill, and with time, water chemistry has generally been improving (Gartner Lee, 1999). It should also be noted that due to progressive monitoring and operations at the site, very little leachate is escaping from the leachate collection and containment systems.

Overall, it has been possible to identify preferred flow paths for groundwater in the area which could aid in determining drilling locations for new monitoring wells. In this instance, it was possible to locate subsurface fractures using electromagnetic, ground-penetrating radar, and geological techniques. With the addition of vertical-dipole azimuthal conductivity data, fracture orientation can be determined.

References

B.C. Environment, 1998. British Columbia Water Quality Guidelines (Criteria); 1998 Edition, prepared by Water Quality Section Management Branch, Environment and Resource Protection Department, MOELP, August 1998.

Best, M.E., and Boniwell, J.B., Eds., 1989. A geophysical handbook for geologists: Special Volume 41, The Canadian Institute of Mining and Metallurgy, Montreal, Quebec, Canada.

Best, M.E., 1989. Electromagnetic Induction methods. *In* A geophysical handbook for geologists. *Edited by* M.E. Best and J.B. Boniwell. The Canadian Institute of Mining and Metallurgy, special volume 41, Canada, pp. 47-53.

Bolshakov, D.K., Modin, I.N., Pervago, E.V., and Shevnin, V.A., 1995. Anisotropy effects investigations in some inhomogeneous media: Proceedings of the European Association of Geoscientists and Engineers (EAGE) 57th Conference and Technical Exhibition, May 29th-June 2nd, 1997, Glasgow, Scotland, P034.

Bolshakov, D.K., Modin, I.N., Pervago, E.V., and Shevnin, V.A., 1997. Separation of anisotropy and inhomogeneity influence by the spectral analysis of azimuthal resistivity diagrams: Proceedings of 3rd Meeting of the Environmental and Engineering Geophysical Society – European Section, September 8th-11th, 1997, Aarhus, Denmark, 147-150.

Davis, J.L., and Annan, A.P. 1989. Ground-penetrating radar for high-resolution mapping of soil and stratigraphy. Geophysical Prospecting, **37**:531-551

Gartner Lee Ltd., 1998a. Hartland Landfill Monitoring Program – 1997 Annual Report. Report prepared for Capital Regional District. GLL 98-753.

Gartner Lee Ltd., 1998b. Hartland Landfill – Geophysical Study. Report prepared for Capital Regional District. GLL 98-753.

Gartner Lee Ltd., 1999. Hartland Landfill Monitoring Program – 1998 Annual Report. Report prepared for Capital Regional District. GLL 99-733.

Grant, F.S., and West, G.F., 1965. Interpretation theory in applied geophysics. McGraw-Hill Book Company, New York.

Kearey, P. and Brooks, M., 1991. An introduction to geophysical exploration. Blackwell Science Ltd., England.

Klein, C. and Hurlbut, C.S., 1993. Manual of Mineralogy. John Wiley & Sons, Inc., New York.

Lomas, N., 1990. Background information – Hartland Landfill site handout, November.

McNeill, J.D., 1980. Electromagnetic terrain conductivity measurement at low induction numbers: Technical Note TN-6, Geonics Limited, Ontario, Canada.

Pervago, E.V., Bolshakov, D.K., Modin, I.N., and Shevnin, V.A., 1997. The new approach to the analysis of the azimuthal resistivity data over anisotropic media: Proceedings of the European Association of Geoscientists and Engineers (EAGE) 59th Conference and Technical Exhibition, May 26th-30th, 1997, Geneva, Switzerland, 139.

Piteau and Associates, 1983. Hydrogeologic evaluation of southern perimeter for Hartland Landfill, Victoria, B.C.

Sandberg, S.K. and Jagel, D.L. 1996. The electromagnetic azimuthal resistivity method. Proceedings of the Symposium on the Application of Geophysics to Engineering and Environmental Problems, April 28th – May 2nd, 1996, Keystone, Colorado. 31-40.

Sandberg, S.K., Fitts, C.R., and Drasdis, J.B., 1996. Hydraulic anisotropy derived from azimuthal resistivity and magnetics. 58th European Association of Geoscientists and Engineers Conference and Technical Exhibition, June 3rd-7th, Amsterdam, The Netherlands.

Sharma, P.V. 1997. Environmental and engineering geophysics. Cambridge University Press, England.

Slater, L.D., Sandberg, S.K., and Janowski, M., 1998. Survey design procedures and data processing techniques applied to the EM azimuthal resistivity method. Journal of Environmental and Engineering Geophysics, **3**:167-178.

Sperling Hansen Associates Inc., 1997. Hartland Landfill Quarry Plan. Report prepared for Capital Regional District. PRJ97004.

Taylor, R.W. and Flemming, A.H., 1988. Characterizing jointed systems by azimuthal resistivity surveys. Groundwater, **26**:464-474.

Telford, W.M., Geldart, L.P., and Sheriff, R.E. 1995. Applied geophysics, second edition. Cambridge University Press, USA.

Ward, S.E. 1990. Resistivity and induced polarization methods. *In* Geotechnical and environmental geophysics. *Edited by* S.E. Ward. Society of Exploration Geophysicists, USA, pp. 147-74.

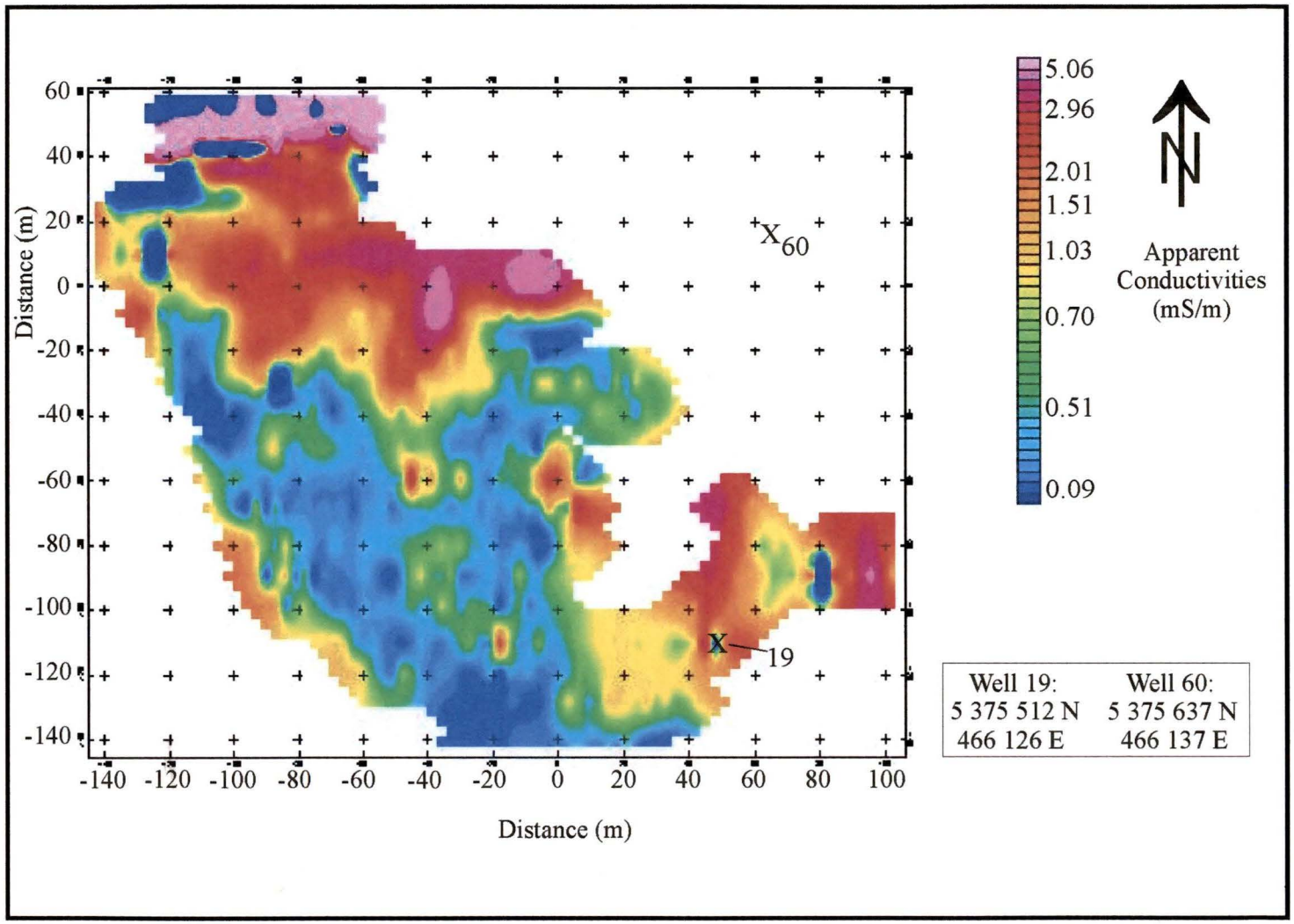

EM contour map which includes data to the east which was omitted from Figure 3.2. Higher conductivity values to the southeast are most likely due to increases in overburden associated with a localized bedrock depression. As reference points, wells 19 and 60 are shown as well as their coordinates.

APPENDIX B

EM Azimuthal plots of apparent conductivities (mS/m) which were not discussed in the text. Some plots show two complete rotations to better investigate noise.

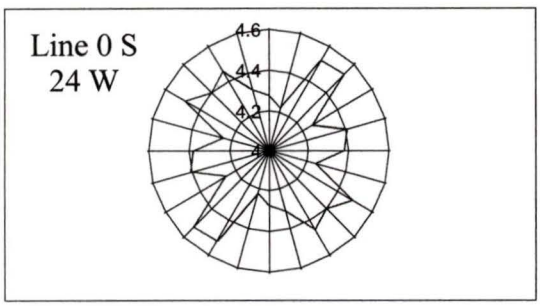

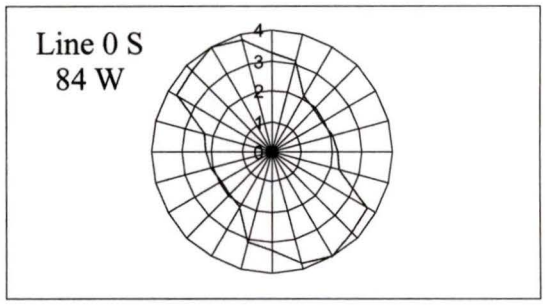

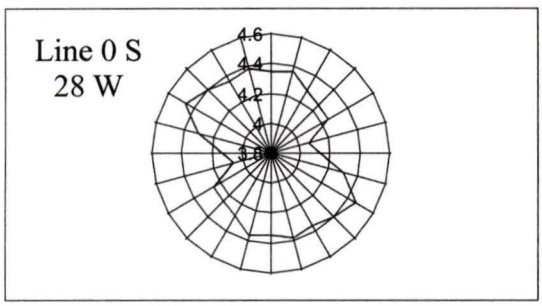

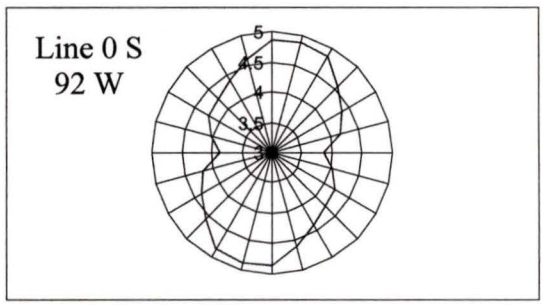

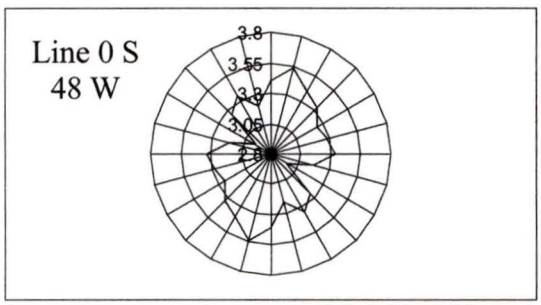

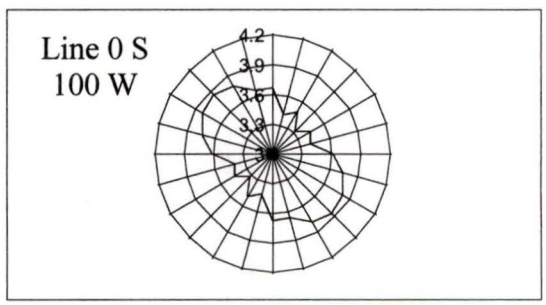

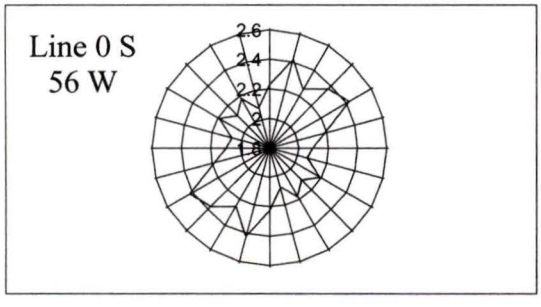

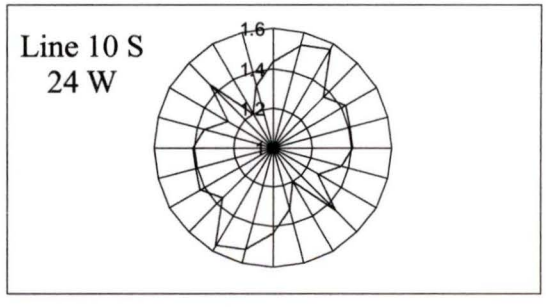

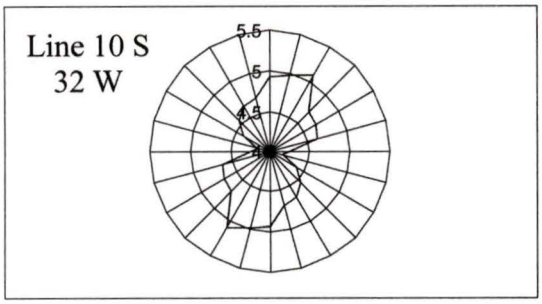
Line 10 S
32 W
5.5
5
4.5

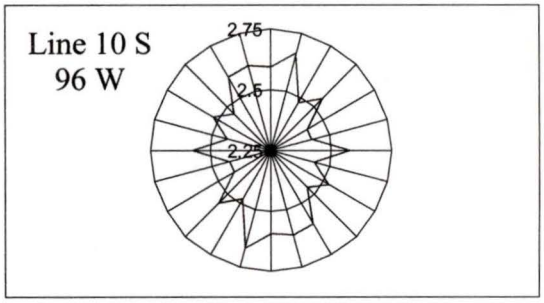
Line 10 S
96 W
2.75
2.5
2.25

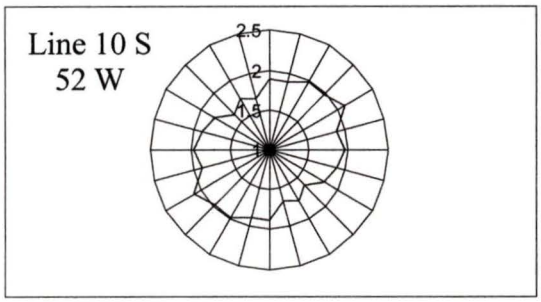
Line 10 S
52 W
2.5
2
1.5

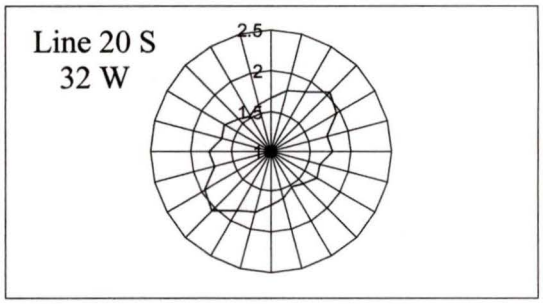
Line 20 S
32 W
2.5
2
1.5

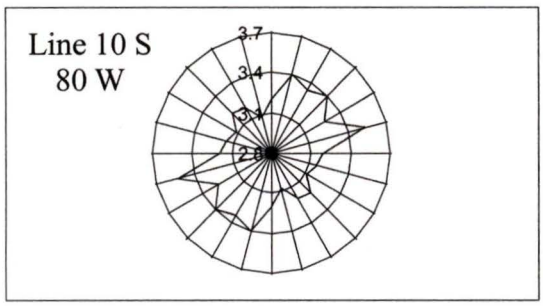
Line 10 S
80 W
3.7
3.4
3.1
2.8

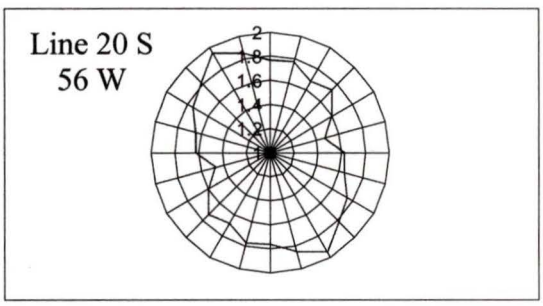
Line 20 S
56 W
2
1.8
1.6
1.4
1.2

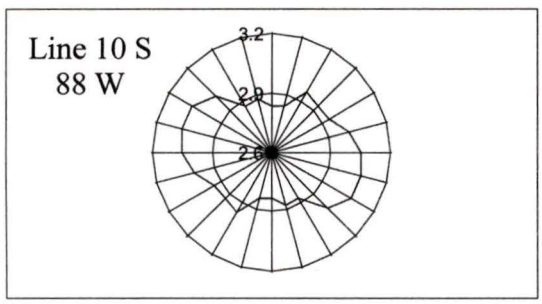
Line 10 S
88 W
3.2
2.9
2.6

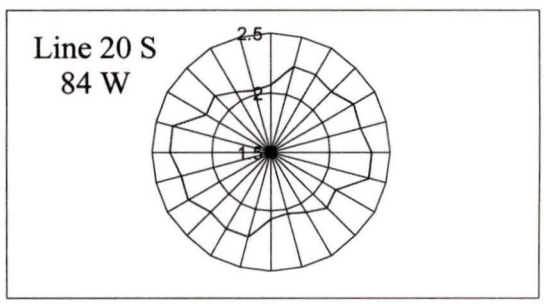
Line 20 S
84 W
2.5
2
1.5

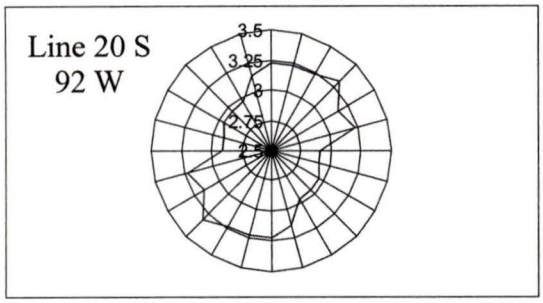
Line 20 S
92 W
3.5
3.25
3
2.75
2.5

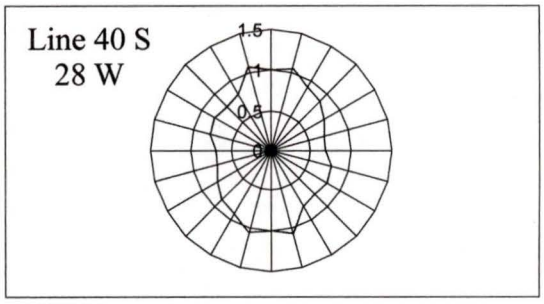
Line 40 S
28 W
1.5
1
0.5
0

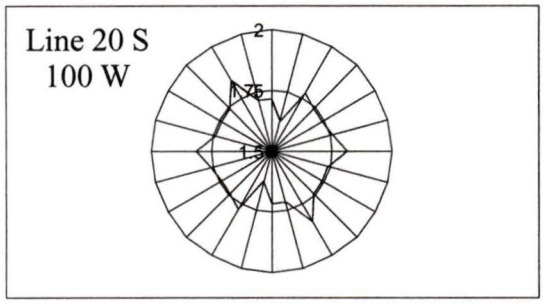
Line 20 S
100 W
2
1.75
1.5

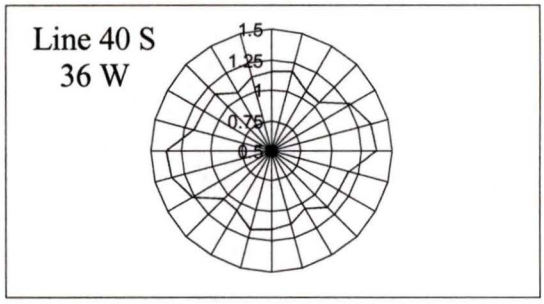
Line 40 S
36 W
1.5
1.25
1
0.75
0.5

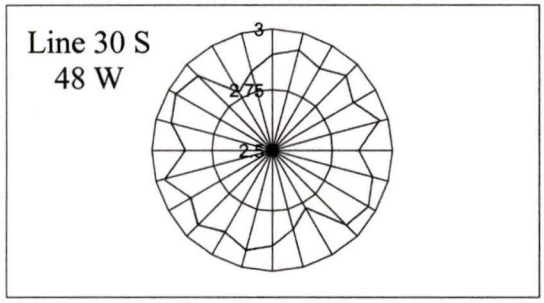
Line 30 S
48 W
3
2.75
2.5

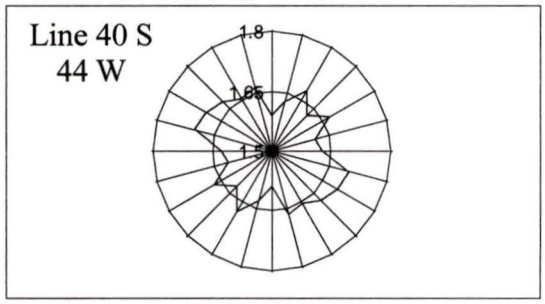
Line 40 S
44 W
1.8
1.65
1.5

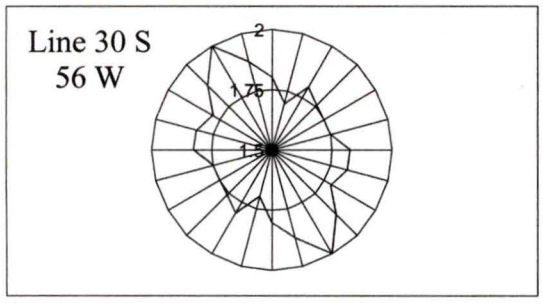
Line 30 S
56 W
2
1.75
1.5

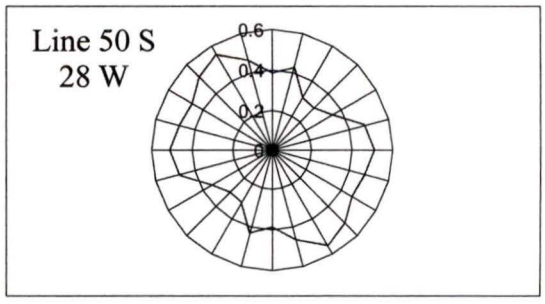
Line 50 S
28 W
0.6
0.4
0.2
0

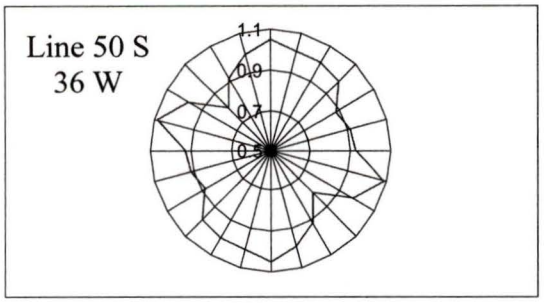
Line 50 S
36 W
1.1
0.9
0.7
0.5

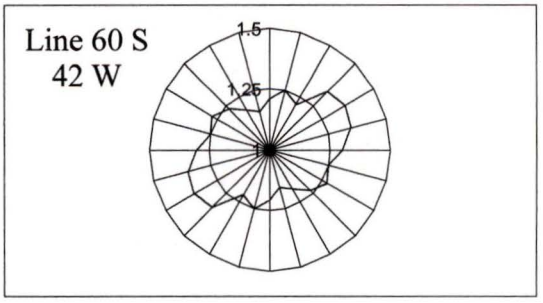
Line 60 S
42 W
1.5
1.25
1

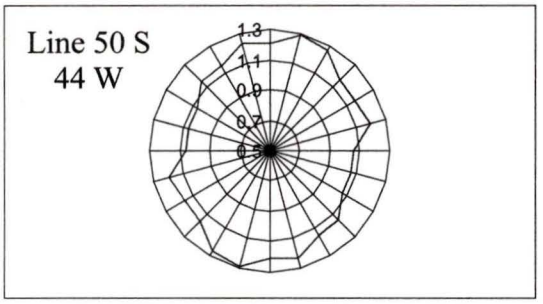
Line 50 S
44 W
1.3
1.1
0.9
0.7
0.5

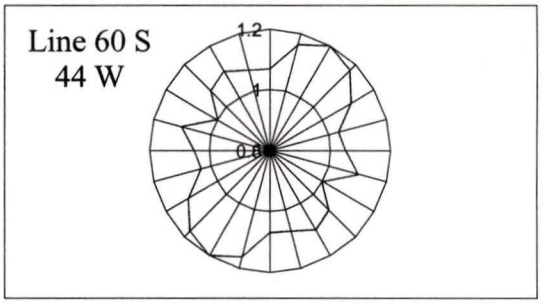
Line 60 S
44 W
1.2
1
0.8

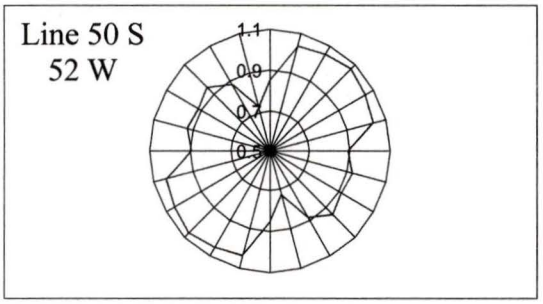
Line 50 S
52 W
1.1
0.9
0.7
0.5

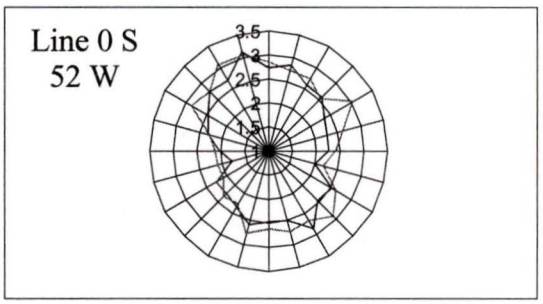
Line 0 S
52 W
3.5
3
2.5
2
1.5
1

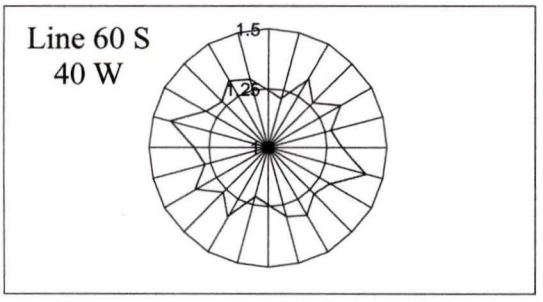
Line 60 S
40 W
1.5
1.25
1

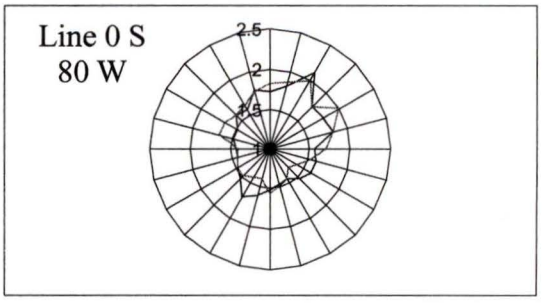
Line 0 S
80 W
2.5
2
1.5
1

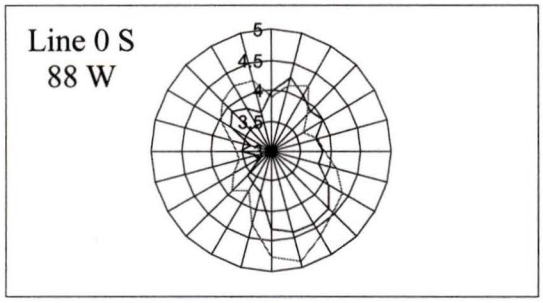
Line 0 S
88 W
5
4.5
4
3.5

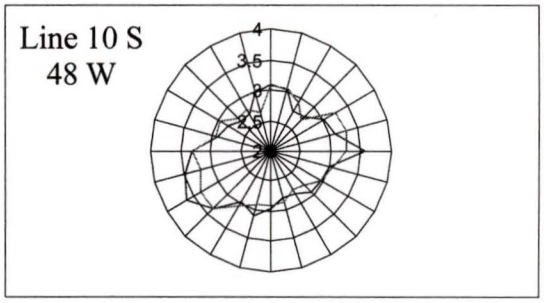
Line 10 S
48 W
4
3.5
3
2.5

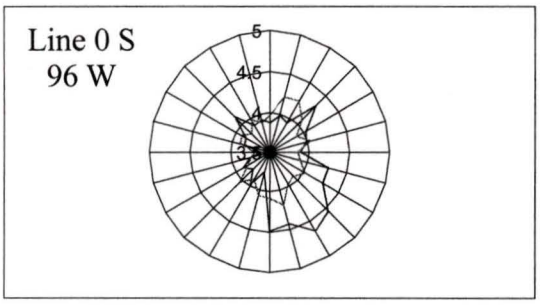
Line 0 S
96 W
5
4.5

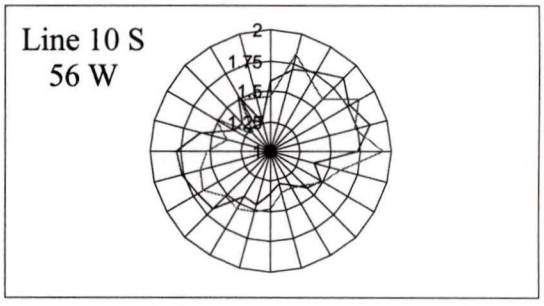
Line 10 S
56 W
2
1.75
1.5
1.25

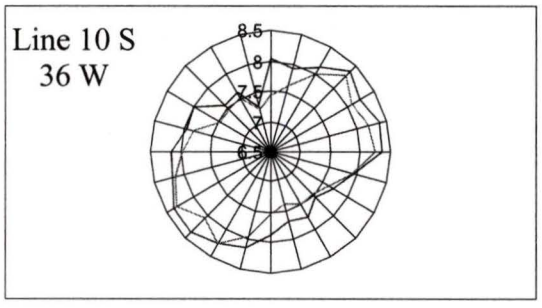
Line 10 S
36 W
8.5
8
7.5
7

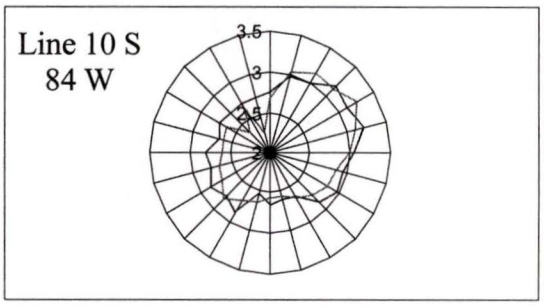
Line 10 S
84 W
3.5
3
2.5

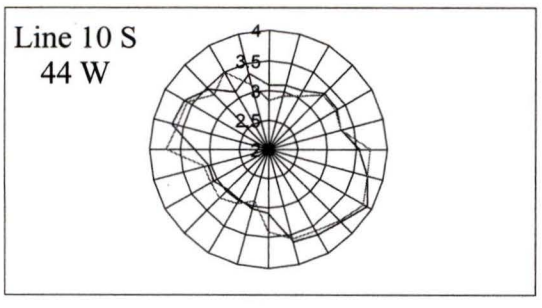
Line 10 S
44 W
4
3.5
3
2.5

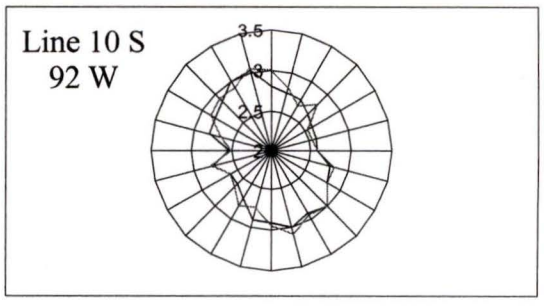
Line 10 S
92 W
3.5
3
2.5

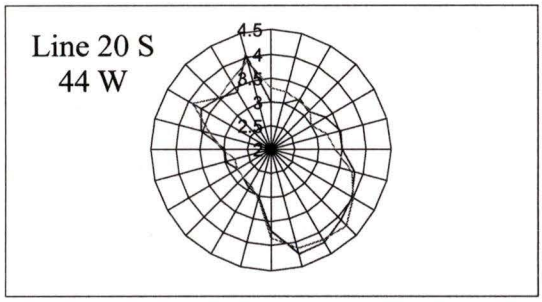
Line 20 S
44 W
4.5
4
3.5
3
2.5

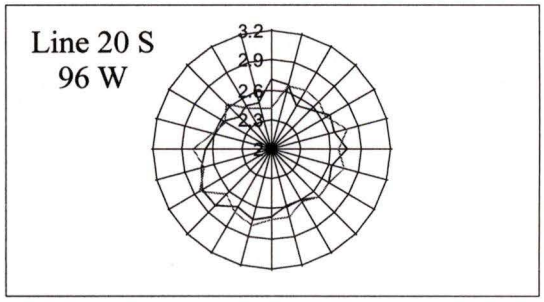
Line 20 S
96 W
3.2
2.9
2.6
2.3

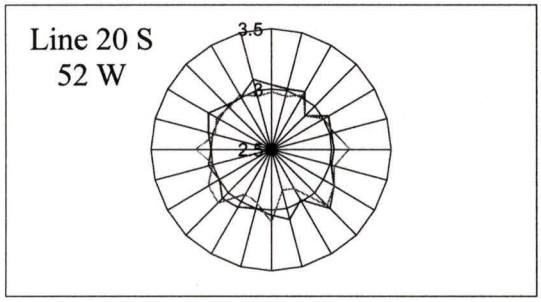
Line 20 S
52 W
3.5
3
2.5

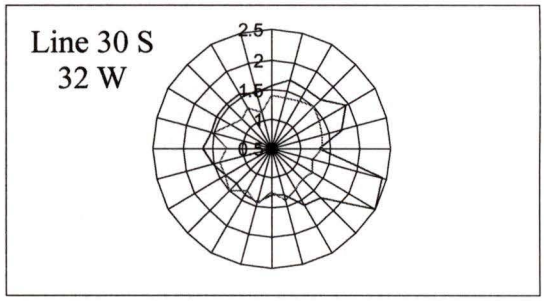
Line 30 S
32 W
2.5
2
1.5
1
0.5

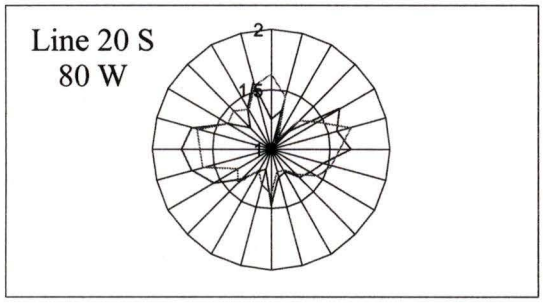
Line 20 S
80 W
2
1.5

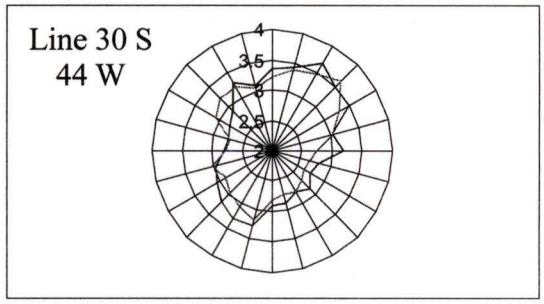
Line 30 S
44 W
4
3.5
3
2.5

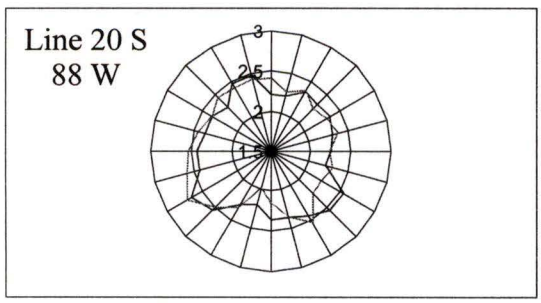
Line 20 S
88 W
3
2.5
2
1.5

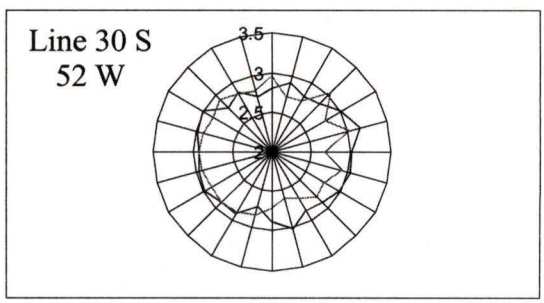
Line 30 S
52 W
3.5
3
2.5

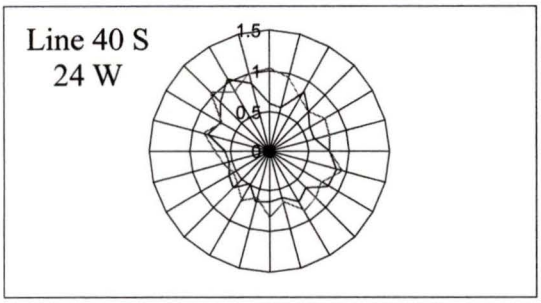
Line 40 S
24 W
1.5
1
0.5
0

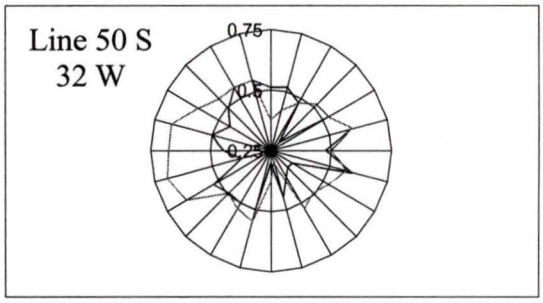
Line 50 S
32 W
0.75
0.5
0.25

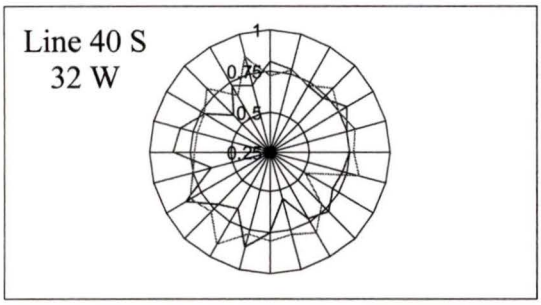
Line 40 S
32 W
1
0.75
0.5
0.25

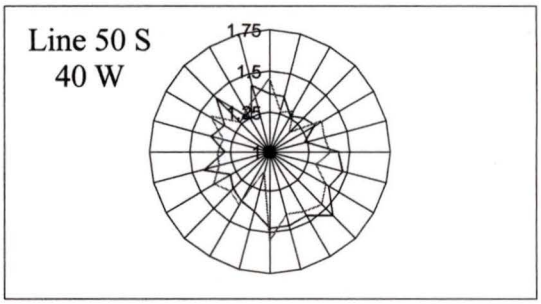
Line 50 S
40 W
1.75
1.5
1.25

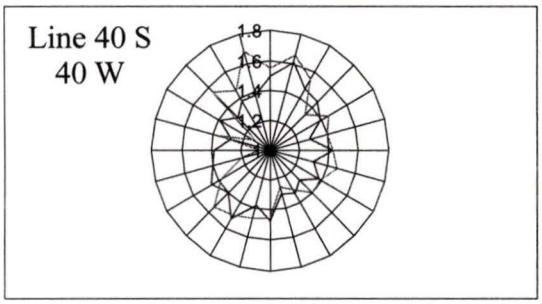
Line 40 S
40 W
1.8
1.6
1.4
1.2
1

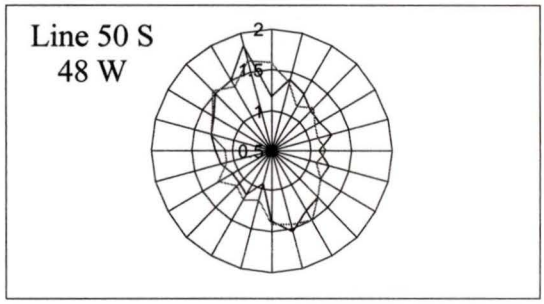
Line 50 S
48 W
2
1.5
1
0.5

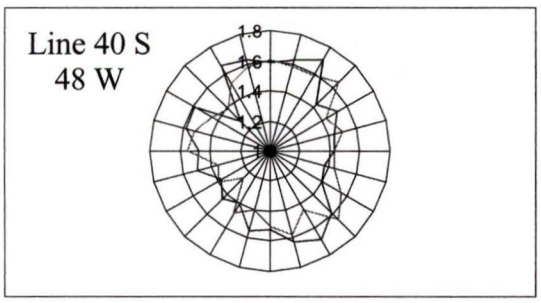
Line 40 S
48 W
1.8
1.6
1.4
1.2
1

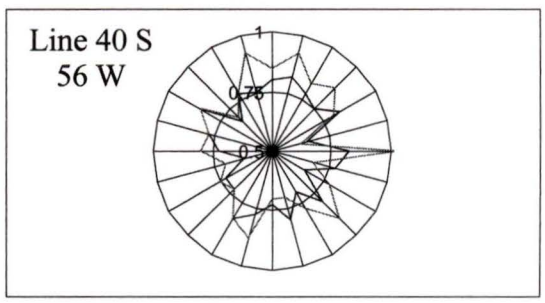
Line 40 S
56 W
1
0.75
0.5

APPENDIX C

Ground-penetrating radar (GPR) profiles not discussed in the text.

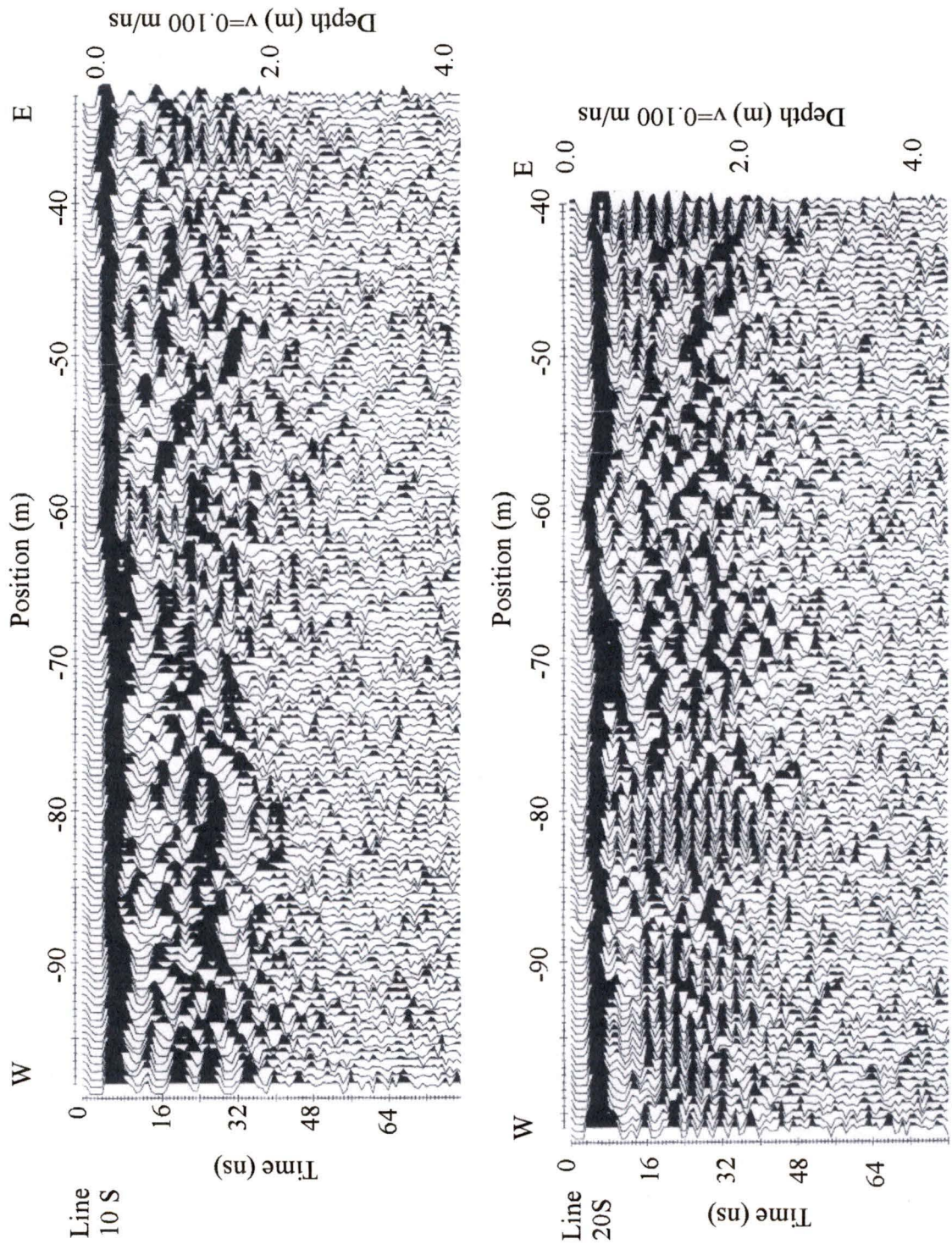

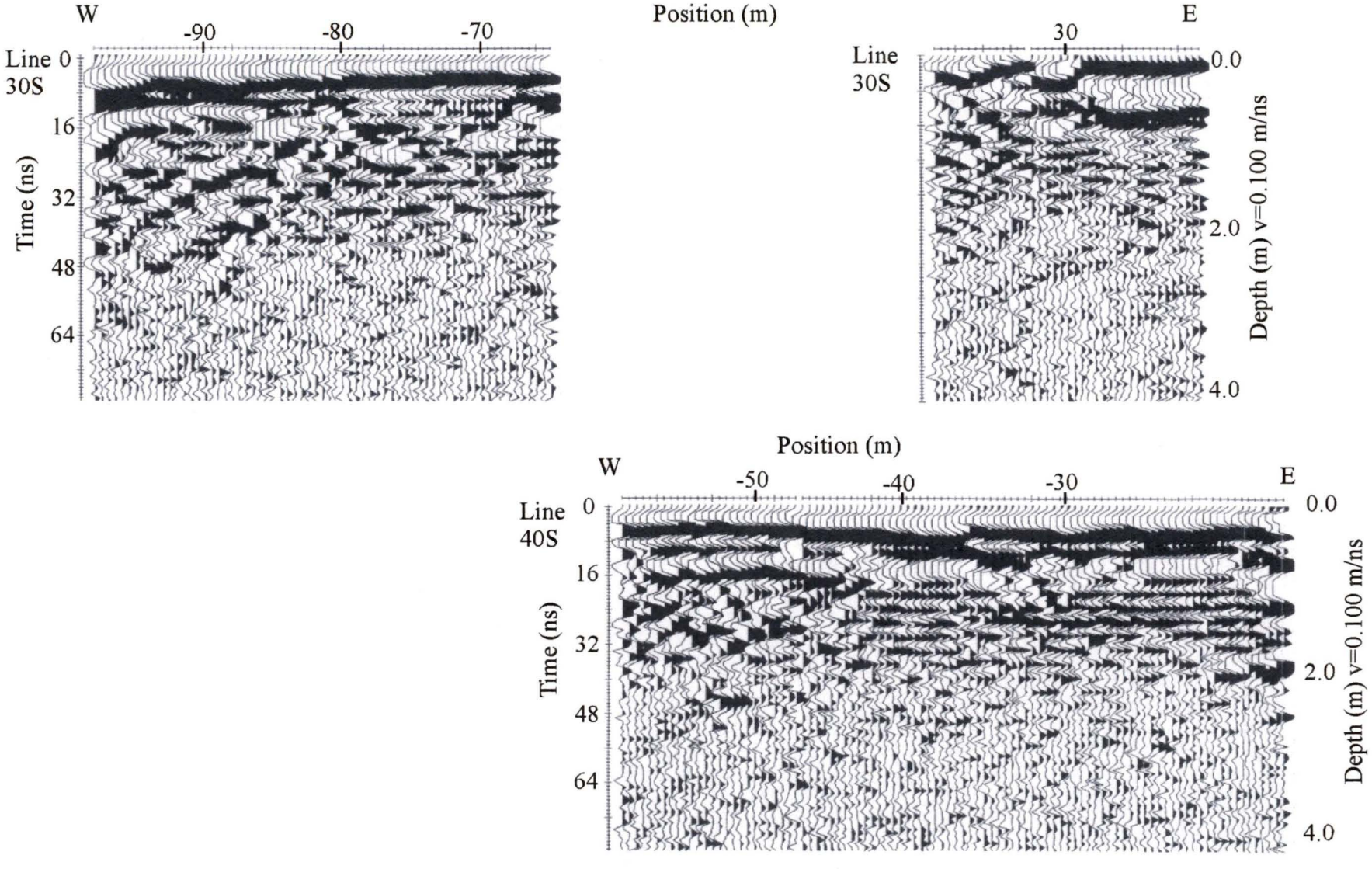
W
-90
-80
-70
Position (m)
Line 0
30S
16
32
48
64
Time (ns)
E
30
Line
30S
0.0
2.0
4.0
Depth (m) v=0.100 m/ns
Position (m)
W
-50
-40
-30
E
Line
40S
0
16
32
48
64
Time (ns)
0.0
2.0
4.0
Depth (m) v=0.100 m/ns

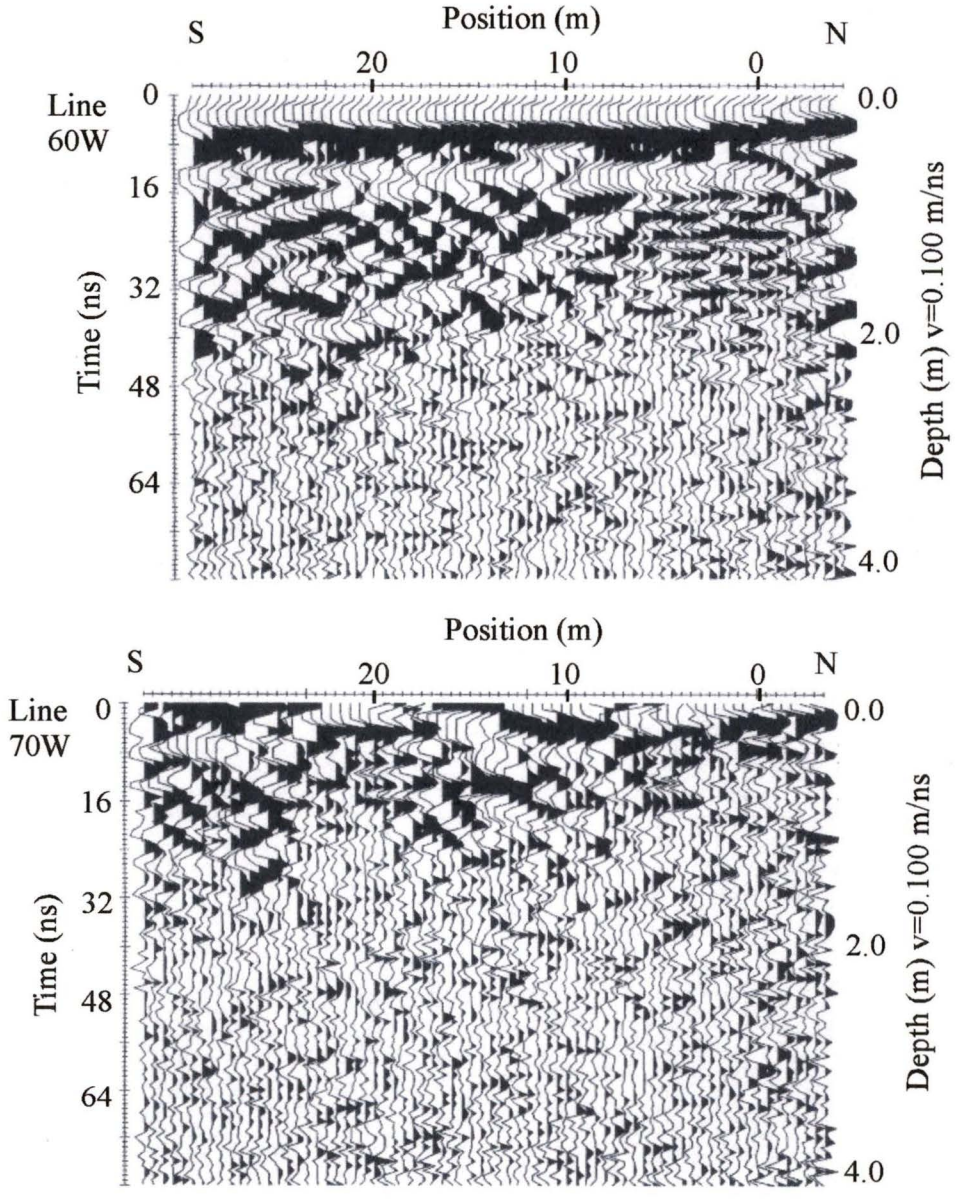
S
Position (m)
N
20
10
0
Line
60W
0
16
32
48
64
Time (ns)
0.0
2.0
4.0
Depth (m) v=0.100 m/ns
S
Position (m)
N
20
10
0
Line
70W
0
16
32
48
64
Time (ns)
0.0
2.0
4.0
Depth (m) v=0.100 m/ns

Common midpoint surveys along 60 W (left) and 70 W (right) used to determine a velocity of 0.100 m/ns.

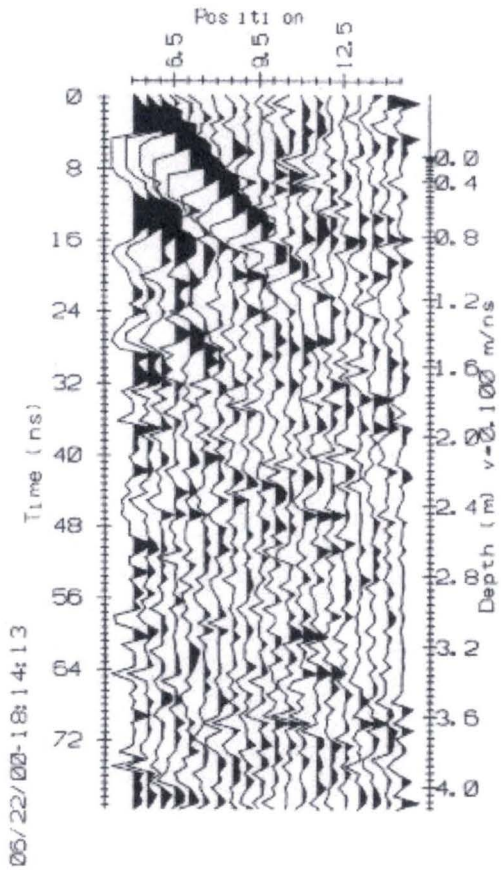

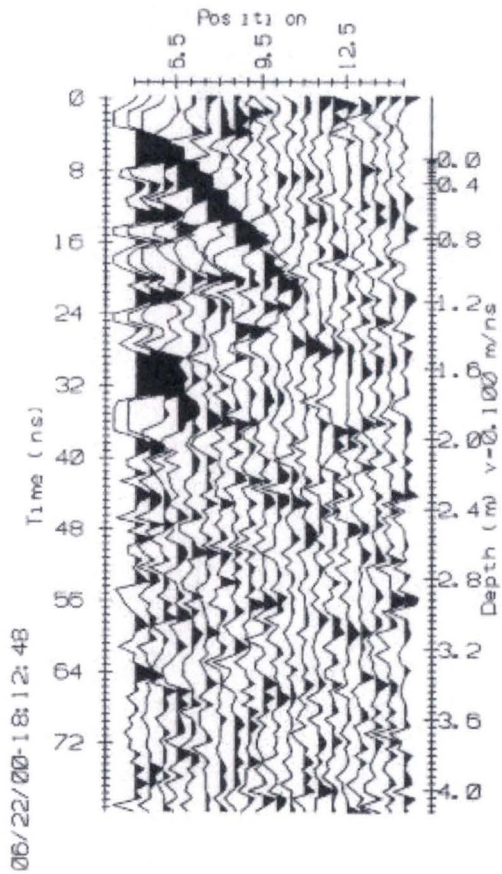

VITA

Surname: Guy Given Names: Gordon Harold James

Place of Birth: Grand Falls, Newfoundland, Canada

Educational Institutions Attended:

University of Victoria	1998 to 2003
Acadia University	1994 to 1998

Degrees Awarded:

BScH	Acadia University	1998

Honours and Awards:

NSERC PGS-A Award	1998 to 2000
University of Victoria President's Research Award	1998 to 2000
LACIR Award	1998

Publications:

Guy, G. 1998. Chemical and textural variations in the Bonnell Brook pluton, Caledonian Highlands, southern New Brunswick, Acadia University.

UNIVERSITY OF VICTORIA PARTIAL COPYRIGHT LICENSE

I hereby grant the right to lend my thesis to users of the University of Victoria Library, and to make single copies only for such users or in response to a request from the Library of any other university, or similar institution, on its behalf or for one of its users. I further agree that permission for extensive copying of this thesis for scholarly purposes may be granted by me or a member of the University designated by me. It is understood that copying or publication of this thesis for financial gain by the University of Victoria shall not be allowed without my written permission.

Title of Thesis:

Relationships of Bedrock Fracturing to Electrical Conductivity and Anisotropy Measurements in a Landfill, Victoria, B.C.

Author: 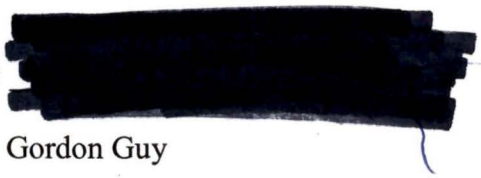

Gordon Guy

April 29, 2003

Note: This license is separate from the non-exclusive license for the National Library of Canada